

Aging dynamics in reentrant ferromagnet: $\text{Cu}_{0.2}\text{Co}_{0.8}\text{Cl}_2\text{-FeCl}_3$ graphite bi-intercalation compound

Masatsugu Suzuki* and Itsuko S. Suzuki

Department of Physics, State University of New York at Binghamton, Binghamton, New York 13902-6000

(Dated: February 6, 2008)

Aging dynamics of a reentrant ferromagnet $\text{Cu}_{0.2}\text{Co}_{0.8}\text{Cl}_2\text{-FeCl}_3$ graphite bi-intercalation compound has been studied using AC and DC magnetic susceptibility. This compound undergoes successive transitions at the transition temperatures T_c ($= 9.7$ K) and T_{RSG} ($= 3.5$ K). The relaxation rate $S(t)$ exhibits a characteristic peak at t_{cr} close to a wait time t_w below T_c , indicating that the aging phenomena occur in both the reentrant spin glass (RSG) phase below T_{RSG} and the ferromagnetic (FM) phase between T_{RSG} and T_c . The relaxation rate $S(t)$ ($= d\chi_{ZFC}(t)/d\ln t$) in the FM phase exhibits two peaks around t_w and a time much shorter than t_w under the positive T -shift aging, indicating a partial rejuvenation of domains. The aging state in the FM phase is fragile against a weak magnetic-field perturbation. The time (t) dependence of $\chi_{ZFC}(t)$ around $t \approx t_{cr}$ is well approximated by a stretched exponential relaxation: $\chi_{ZFC}(t) \approx \exp[-(t/\tau)^{1-n}]$. The exponent n depends on t_w , T , and H . The relaxation time τ ($\approx t_{cr}$) exhibits a local maximum around 5 K, reflecting a chaotic nature of the FM phase. It drastically increases with decreasing temperature below T_{RSG} .

PACS numbers: 75.50.Lk, 75.40.Gb, 75.70.Cn, 75.10.Nr

I. INTRODUCTION

In random spin systems with competing ferromagnetic and antiferromagnetic interactions, the spin frustration effect occurs, leading to a spin-glass (SG) phase at low temperatures. This situation may change when there is a majority of the ferromagnetic interactions and a minority of the antiferromagnetic interactions to create substantial spin frustration effect. The system (so-called reentrant ferromagnet) exhibits two phase transitions at T_{RSG} and T_c ($T_c > T_{RSG}$): the reentrant spin glass (RSG) phase below T_{RSG} and the ferromagnetic (FM) phase between T_{RSG} and T_c . Experimental studies on the dynamic magnetic properties have been carried out for reentrant ferromagnets such as $(\text{Fe}_{0.20}\text{Ni}_{0.80})_{75}\text{P}_{16}\text{B}_6\text{Al}_3$,^{1,2,3,4} $\text{Cr}_{78}\text{Fe}_{22}$,⁵ $(\text{Fe}_{0.65}\text{Ni}_{0.35})_{0.882}\text{Mn}_{0.118}$,⁶ $\text{CdCr}_{2x}\text{In}_{2(1-x)}\text{S}_4$ ($x = 0.90, 0.95$, and 1.00),^{7,8,9} and $\text{Fe}_{0.7}\text{Al}_{0.3}$.¹⁰ For $\text{Cr}_{78}\text{Fe}_{22}$,⁵ $(\text{Fe}_{0.65}\text{Ni}_{0.35})_{0.882}\text{Mn}_{0.118}$,⁶ and $\text{Fe}_{0.7}\text{Al}_{0.3}$,¹⁰ the RSG phase exhibits aging phenomena, which are very similar to those observed in the SG phase of SG systems. No aging phenomenon has been observed in the FM phase. For $(\text{Fe}_{0.20}\text{Ni}_{0.80})_{75}\text{P}_{16}\text{B}_6\text{Al}_3$,^{1,2,3,4} in contrast, not only the RSG phase but also the FM phase exhibit aging phenomena. A strikingly increased fragility to the magnitude of the magnetic field is observed when passing from the low-temperature RSG region into the FM phase, implying a chaotic nature of the FM phase. The effect of the probing field H on the relaxation rate has to be carefully considered. The dramatic decrease of the limiting field around T_{RSG} may explain why other experiments on reentrant ferromagnets have not resolved an aging behavior in the FM phase. For $\text{CdCr}_{2x}\text{In}_{2(1-x)}\text{S}_4$ with $x = 0.90, 0.95$, and 1.0 ,^{7,8,9} the aging behavior of the low frequency AC susceptibility (absorption χ'') is observed both in the FM and RSG phases.

Experimental studies on the aging dynamics have been limited to a macroscopic measurement such as the time evolution of zero-field cooled susceptibility, thermomagnetic susceptibility, and the absorption of the AC magnetic susceptibility. Recently Motoya et al.¹⁰ have studied time-resolved small angle neutron scattering on $\text{Fe}_{0.70}\text{Al}_{0.30}$ in order to probe the microscopic mechanism of slow dynamics. The Lorentzian form of the scattering pattern and the temperature variation of the inverse correlation length below T_{RSG} show that the system is composed of only finite-sized clusters. The size of the clusters gradually decreases with decreasing temperature.

$\text{Cu}_{0.2}\text{Co}_{0.8}\text{Cl}_2\text{-FeCl}_3$ graphite bi-intercalation compound (GBIC) is one of typical 3D Ising reentrant ferromagnets. It has a unique layered structure where the $\text{Cu}_{0.2}\text{Co}_{0.8}\text{Cl}_2$ intercalate layer ($= I_1$) and FeCl_3 intercalate layers ($= I_2$) alternate with a single graphite layer (G), forming a stacking sequence ($-G-I_1-G-I_2-G-I_1-G-I_2-G-\dots$) along the c axis. In the $\text{Cu}_{0.2}\text{Co}_{0.8}\text{Cl}_2$ intercalate layer, two kinds of magnetic ions (Cu^{2+} and Co^{2+}) are randomly distributed on the triangular lattice. The static and dynamic magnetic properties have been reported in a previous paper.¹¹ This compound undergoes successive transitions at the transition temperatures T_c ($= 9.7$ K) and T_{RSG} ($= 3.5$ K). A prominent nonlinear susceptibility is observed between T_{RSG} and T_c , suggesting a chaotic nature of the FM phase.

In this paper we report our experimental study on the aging dynamics of the RSG and FM phases of $\text{Cu}_{0.2}\text{Co}_{0.8}\text{Cl}_2\text{-FeCl}_3$ GBIC using DC and AC magnetic susceptibility measurements. Our system is cooled from 50 K to T ($< T_c$) in the absence of an external magnetic field. This ZFC aging protocol process is completed at $t_a = 0$, where t_a is defined as an age (the total time after the ZFC aging protocol process). Then the system is aged at T under $H = 0$ until $t_a = t_w$, where t_w is a wait time.

The aging behavior of the ZFC magnetic susceptibility $\chi_{ZFC}(t)$ has been measured under the various aging processes: (i) a wait time t_w ($2.0 \times 10^3 \leq t \leq 3.0 \times 10^4$ sec), T ($1.9 \leq T \leq 9$ K), and H ($1 \leq H \leq 60$ Oe) as parameters, and (ii) the T -shift and H -shift perturbations. The relaxation rate defined by $S(t) = d\chi_{ZFC}/d\ln t$ (see Sec. II A for the definition) exhibits a peak at a characteristic time t_{cr} close to t_w below T_c , indicating the occurrence of the aging phenomena both in the RSG and FM phases. We will also show that the t dependence of $\chi_{ZFC}(t)$ around $t \approx t_w$ is well described by a stretched exponential relaxation [$\chi_{ZFC}(t) \approx \exp[-(t/\tau)^{1-n}]$] (see Sec. II B), where n is an exponent and τ is a relaxation time nearly equal to t_{cr} . We will show that n , τ , and t_{cr} depend on T , t_w , and H . The local maximum of τ and t_{cr} around 5 K is observed, reflecting the chaotic nature of the FM phase. A partial rejuvenation of the system occurs in $S(t)$ under the positive shift in the FM phase.

II. BACKGROUND

A. Scaling form of $\chi_{ZFC}(t_w; t + t_w)$ and $\chi''(\omega, t)$ in the SG phase

After the SG system is cooled to T ($< T_{SG}$) through the ZFC aging protocol at $t_a = 0$, the size of domain defined by $R_T(t_a)$ grows with the age of t_a and reaches $R_T(t_w)$ just before the field is turned on at $t = 0$ or $t_a = t_w$.¹² The aging behavior in χ_{ZFC} is observed as a function of the observation time t . After $t = 0$, a probing length $L_T(t, t_w)$ corresponding to the maximum size of excitation grows with t , in a similar way as $R_T(t_a)$. The quasi-equilibrium relaxation occurs first through local spin arrangements in length $L_T(t, t_w) \ll R_T(t_w)$, followed by non-equilibrium relaxation due to domain growth, when $L_T(t, t_w) \approx R_T(t_w)$, so that a crossover between the short-time quasi-equilibrium decay and the non-equilibrium decay at longer observation times is expected to occur near $t \approx t_w$. The droplet model¹³ predicts the following two. (i) The equilibrium SG states at two temperatures with the difference ΔT are uncorrelated when the overlap length $L_{\Delta T}$ is smaller than $R_T(t_w)$, i.e., so-called temperature (T)-chaos nature of the SG phase. (ii) The equilibrium SG states at two fields with the difference ΔH are uncorrelated when the overlap length $L_{\Delta H}$ is smaller than $R_T(t_w)$.

The absorption χ'' of the AC magnetic susceptibility is evaluated from the spin auto-correlation function $C(t_a - t; t_a) = \langle S_i(t_a - t) S_i(t_a) \rangle$ using the fluctuation-dissipation theorem (FDT) as^{14,15,16,17}

$$\chi''(\Delta t_w; t + \Delta t_w) \approx (-\pi/2T) \partial C(\Delta t_w; t + \Delta t_w) / \partial \ln t, \quad (1)$$

where $t_a = t + \Delta t_w$, $\Delta t_w = 2\pi/\omega$ (typically $\Delta t_w \leq 10^2$ sec), ω is the angular frequency, and t is much larger than Δt_w . In the auto-correlation function, the over-line denotes the average over sites and over different realizations of bond disorder, and the bracket denotes the average

over thermal noises. For slow processes, the dispersion $\chi'(\Delta t_w; t + \Delta t_w)$ is approximated by

$$\chi'(\Delta t_w; t + \Delta t_w) \approx [1 - C(\Delta t_w; t + \Delta t_w)]/T. \quad (2)$$

In the quasi-equilibrium regime where the FDT holds, the ZFC susceptibility $\chi_{ZFC}(t_w; t + t_w)$ is described by

$$\chi_{ZFC}(t_w; t + t_w) \approx [1 - C(t_w; t + t_w)]/T, \quad (3)$$

where $t_a = t + t_w$ and t_w is a wait time. Then the relaxation rate $S(t)$ is described by

$$\begin{aligned} S(t) &= d\chi_{ZFC}(t_w; t + t_w) d\ln t \\ &= (-1/T) \partial C(t_w; t + t_w) / \partial \ln t, \end{aligned} \quad (4)$$

which corresponds to $(2/\pi)\chi''(t_w; t + t_w)$. In spin glasses the aging manifests by the fact that $C(t_w; t_w + t)$ shows a strong dependence on the value of t_w .

It is predicted that $C(t_w; t + t_w)$ can be described by an addition of the short-time and long-time contributions¹⁷

$$C(t_w; t + t_w) \approx C_{eq}(t) + C_{ag}(t_w; t + t_w), \quad (5)$$

whereas the aging at the SG transition temperature T_{SG} leads to a multiplicative representation,

$$C(t_w; t + t_w) \approx C_{eq}(t) C_{ag}(t_w; t + t_w). \quad (6)$$

Here the equilibrium part can be described by power-law form

$$C_{eq}(t) \approx t^{-\alpha}, \quad (7)$$

with a temperature-dependent exponent α (≈ 0). These two forms (additive and multiplicative representations) are actually not so different for short times, since $C_{ag}(t_w; t + t_w)$ is approximately constant for $t \ll t_w$, in the regime where $C_{eq}(t)$ varies most.

The ZFC susceptibility is described by either an additive form

$$\chi_{ZFC}(t_w; t + t_w) \approx (1/T) [1 - C_{eq}(t) - C_{ag}(t_w; t + t_w)], \quad (8)$$

or a multiplicative form

$$\begin{aligned} \chi_{ZFC}(t) &= \chi_{ZFC}(t_w; t + t_w) \\ &\approx (1/T) [1 - C_{eq}(t) C_{ag}(t_w; t + t_w)]. \end{aligned} \quad (9)$$

When the additive form of C is used, the absorption $\chi''(\omega, t)$ can be rewritten as

$$\chi''(\omega, t) = \chi''_{eq}(t) + \chi''_{ag}(\omega, t), \quad (10)$$

where

$$\chi''_{ag}(\omega, t) = (-\pi/2T) \partial C_{ag}(\Delta t_w; t + \Delta t_w) / \partial \ln t, \quad (11)$$

and

$$\chi''_{eq}(t) = (-\pi/2T) \partial C_{eq}(t) / \partial \ln t \approx t^{-\alpha}. \quad (12)$$

Here we assume that the aging contribution $C_{ag}(t_w; t + t_w)$ is approximated by a scaling function of t/t_w as¹⁷

$$C_{ag}(t_w; t + t_w) = F(t/t_w). \quad (13)$$

In Eq.(10) the first term $\chi''_{eq}(t) [\approx t^{-\alpha}]$ is independent of ω , while the second term $\chi''_{ag}(\omega t) [\approx (\omega t)^{-b}]$ is a function of ωt (see Sec. IV F for detail). Here α (≈ 0) and b (≈ 0.2) are exponents of quasi-equilibrium part and aging parts. In all cases we observe a slow time decay (aging) of $\chi''(\omega, t)$ towards an asymptotic frequency dependent value $\chi''(\omega, T)$ (stationary susceptibility):

$$\chi''(\omega, t) \rightarrow \chi''(\omega, T) \approx \omega^\alpha, \quad (14)$$

in the limit of $\omega t \rightarrow \infty$, where $\chi''_{ag}(\omega t)$ is assumed to be zero.

B. Stretched exponential relaxation in the SG phase

Here we present a simple review on the stretched exponential relaxation of χ_{ZFC} of SG phase after the ZFC aging protocol. Theoretically^{18,19} and experimentally^{20,21,22,23,24,25,26,27,28,29,30} it has been accepted that the time variation of $\chi_{ZFC}(t)$ may be described by a product of a power-law form and a stretched exponential function

$$\chi_{ZFC}(t) = M_{ZFC}(t)/H = \chi_0 - At^{-m} \exp[-(t/\tau)^{1-n}], \quad (15)$$

where the exponent m may be positive and is very close to zero, n is between 0 and 1, τ is a characteristic relaxation time, and χ_0 and A are constants. In general, these parameters are dependent on t_w . This form of $\chi_{ZFC}(t)$ incorporates both the nonequilibrium aging effect through the stretched exponential factor $[\exp[-(t/\tau)^{1-n}]]$ in the crossover region ($t \approx t_w$ and $t > t_w$) between the quasi equilibrium state and nonequilibrium state, and an equilibrium relaxation response at $t \ll t_w$ through a pure power-law relaxation (t^{-m}). Note that Ogielski¹⁸ fits his data by a stretched exponential multiplied by a power function. For $0.6 < T/T_{SG} < 1$, Ogielski¹⁸ fits it by a power law with a different temperature dependence of exponent m . When $t \ll \tau$, $\chi_{ZFC}(t)$ is well described by a power law form given by At^{-m} . However, in the regime of $t \approx \tau$, the stretched exponential relaxation is a very good approximation in spite of finite m that is very small.

For all temperatures, $\chi_{ZFC}(t)$ increases with increasing t and the relaxation rate $S(t)$, which is defined by

$$S(t) = d\chi_{ZFC}(t)/d \ln t = t d\chi_{ZFC}(t)/dt, \quad (16)$$

exhibits a maximum at t_{cr} that is close to t_w . Using Eq.(15) for $\chi_{ZFC}(t)$, the relaxation rate $S(t)$ can be derived as

$$S(t) = -(A\tau^{-m}) \exp[-(t/\tau)^{1-n}] (t/\tau)^{-(m+n)} [(1-n) + m(t/\tau)^{n-1}]. \quad (17)$$

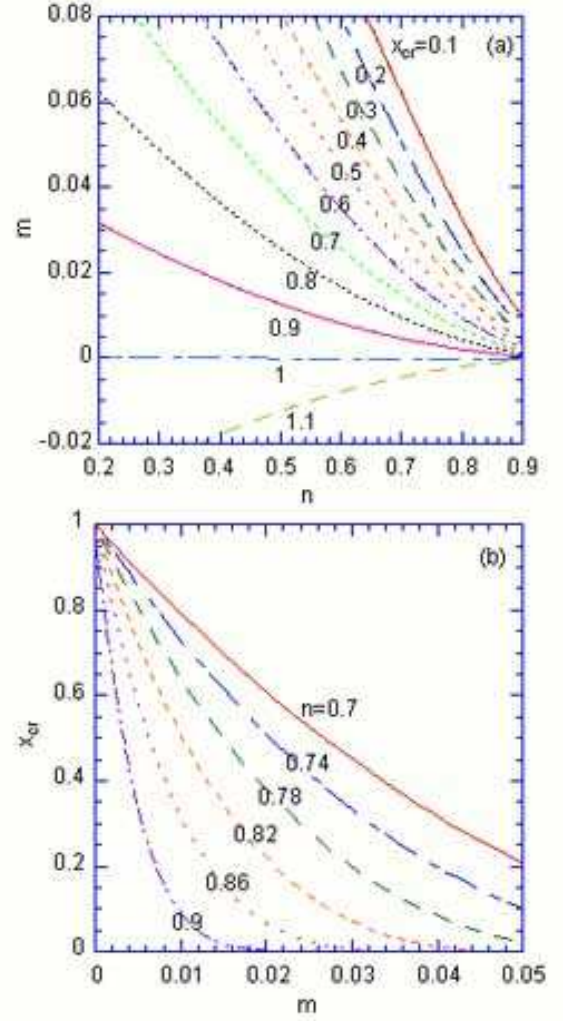


FIG. 1: (Color online)(a) Contour plot of x_{cr} ($0.1 \leq x_{cr} \leq 1.1$) in the (n, m) plane, where $x_{cr} = t_{cr}/\tau$, and the points with the same x_{cr} are connected by the same solid line. The definition of t_{cr} and τ is given in the text. (b) Plot of x_{cr} vs m at various n . The expression for x_{cr} is given by Eqs.(19) and (20).

The condition that $S(t)$ may have a peak at $t = t_{cr}$ [$dS(t)/dt = 0$] leads to the ratio $x_{cr} = t_{cr}/\tau$ satisfying the following equation

$$(1-n)^2 x_{cr}^2 - (1-n)(1-2m-n)x_{cr}^{n+1} + m^2 x_{cr}^{2n} = 0. \quad (18)$$

The solution of Eq.(18) can be exactly obtained as

$$x_{cr} = t_{cr}/\tau = (\xi/2)^{1/(1-n)}, \quad (19)$$

with

$$\xi = [1-2m-n+(1-n)^{1/2}(1-4m-n)^{1/2}]/(1-n), \quad (20)$$

where $4m+n < 1$. Note that the value of x_{cr} is uniquely determined only by the values of n and m . When $m = 0$, $x_{cr} = 1$ (or $t_{cr} = \tau$), which is independent of n . Figure

1(a) shows the contour plot of x_{cr} in the (n, m) plane with $-0.02 \leq m \leq 0.08$ and $0.2 \leq n \leq 0.9$, where the points having the same x_{cr} are connected by each solid line. The value of x_{cr} is lower than 1 for $m > 0$, is equal to 1 for $m = 0$ irrespective of n , and is larger than 1 for $m < 0$. Figure 1(b) shows a plot of x_{cr} as a function of m at various fixed n . The maximum value of $S(t)$ at $t = t_{cr}$ is given by

$$S_{\max} = A\tau^{-m}2^{-1+\frac{m}{1-n}} \exp\left[-\frac{1}{2} + \frac{m}{1-n} - \frac{\sqrt{1-4m-n}}{2\sqrt{1-n}}\right](1-n)^{\frac{m}{1-n}} \times (1-n + \sqrt{1-n}\sqrt{1-4m-n}) \times (1-2m-n + \sqrt{1-n}\sqrt{1-4m-n})^{\frac{-m}{1-n}}. \quad (21)$$

When $m = 0$, S_{\max} is equal to $S_{\max}^0 [= A(1-n)/e]$ with $e = 2.7182$.

III. EXPERIMENTAL PROCEDURE

We used the same sample of $\text{Cu}_{0.2}\text{Co}_{0.8}\text{Cl}_2\text{-FeCl}_3$ GBIC that was used in the previous paper.¹¹ The detail of the sample characterization and synthesis were presented in the references of the previous paper.¹¹ The DC magnetization and AC susceptibility of $\text{Cu}_{0.2}\text{Co}_{0.8}\text{Cl}_2\text{-FeCl}_3$ GBIC were measured using a SQUID magnetometer (Quantum Design, MPMS XL-5) with an ultra low field capability option. The remnant magnetic field was reduced to zero field (exactly less than 3 mOe) at 298 K for both DC magnetization and AC susceptibility measurements. The AC magnetic field used in the present experiment has a peak magnitude of the AC field (h) and a frequency $f = \omega/2\pi$. Each experimental procedure for measurements is presented in the text and figure captions.

In our measurement of the time (t) dependence of the zero-field cooled (ZFC) magnetization (M_{ZFC}), the time required for the ZFC aging protocol and subsequent wait time were precisely controlled. Typically it takes 240 ± 3 sec to cool the system from 10 K to T ($< T_c$). It takes another 230 ± 3 sec until T becomes stable within the uncertainty (± 0.01 K). The system is kept at T and $H = 0$ for a wait time t_w (typically $t_w = 1.5 \times 10^4$ or 3.0×10^4 sec). At time $t = 0$, external magnetic field H is applied along any direction perpendicular to the c axis. The time for setting up a magnetic field from $H = 0$ to $H = 1$ Oe is 68 ± 2 sec. In the ZFC measurement, the sample is slowly moved through the pick-up coils over the scan length (4 cm). The magnetic moment of the sample induces a magnetic flux change in the pick-up coils. It takes 12 sec for each scan. The data at t is regarded as the average of M_{ZFC} measured over the scanning time t_s between the times $t - (t_s/2)$ and $t + (t_s/2)$. Thus the time window Δt is a scanning time (t_s). The measurement was carried out at every interval of $t_s + t_p$, where t_p is a pause between consecutive measurements. Typically we used

(i) the time window $\Delta t = 36$ sec for the measurements with three scans and $t_p = 45$ sec or 30 sec, and (ii) the time window $\Delta t = 12$ sec for the measurements with one scan and $t_p = 1$ or 2 sec.

IV. RESULT

A. $\chi''(\omega, T)$ and $\chi_{ZFC}(T)$

In the previous paper¹¹ the magnetic properties of $\text{Cu}_{0.2}\text{Co}_{0.8}\text{Cl}_2\text{-FeCl}_3$ GBIC have been extensively studied from our results on DC susceptibility (χ_{ZFC} , χ_{FC}), and AC magnetic susceptibility (χ' and χ''). In Fig. 2(a), as a typical example we show the T dependence of the absorption $\chi''(\omega, T)$ at various f , where $h = 50$ mOe. It is concluded from this figure that our system undergoes two phase transitions at $T_{RSG} = 3.5$ K and $T_c = 9.7$ K. There are a RSG phase below T_{RSG} and an FM phase between T_{RSG} and T_c .

In order to demonstrate the evidence of aging behavior in χ_{ZFC} , we measured the T dependence of χ_{ZFC} ($= M_{ZFC}/H$) in the following two ZFC protocols. The system was quenched from 50 to 1.9 K in the absence of H before the measurement. The susceptibility χ_{ZFC} was measured with increasing T from 1.9 K to $T_1 = 7.0$ K in the presence of H ($= 1$ Oe), where T_1 is in the FM phase. The system was kept at T_1 for a wait time $t_{w1} = 1.5 \times 10^4$ sec. Subsequently χ_{ZFC} was measured with further increasing T from T_1 to 20 K. The system was annealed at 50 K for 1.2×10^3 sec in the presence of H ($= 1$ Oe). The susceptibility χ_{FC} was continuously measured from 20 to 1.9 K. In Fig. 2(b) we show the T dependence of χ_{ZFC} and χ_{FC} ($H = 1$ Oe) thus obtained (denoted as the ZFC-1 and FC-1 processes). We find that there is a remarkable increase of χ_{ZFC} with increasing t during the one stop at $T_1 = 7.0$ K. As T again increases from T_1 , χ_{ZFC} starts to decrease with increasing T and merges with χ_{ZFC}^{ref} without the stop as a reference at $T \approx 7.3$ K (see the inset of Fig. 2(b)). The state at $T = 7.3$ K is uncorrelated with that at T_1 since the temperature difference ΔT is large so that the domain size $R_{T1}(t_{w1})$ is much larger than the overlap length $L_{\Delta T}$.

In another measurement (denoted as the ZFC-2 and FC-2 processes), the system was kept at $T_2 = 3.5$ K in the RSG phase for $t_{w2} = 1.5 \times 10^4$ sec during the ZFC process. In the inset of Fig. 2(b) we show the T dependence of χ_{ZFC} in the ZFC-2 process. There is a remarkable increase of χ_{ZFC} during the one stop at T_2 . As T again increases from T_2 , χ_{ZFC} starts to increase with a derivative $d\chi_{ZFC}/dT$ that is positive and much smaller than that of χ_{ZFC}^{ref} . This susceptibility χ_{ZFC} merges with χ_{ZFC}^{ref} at $T \approx 3.9$ K. The state at $T = 3.9$ K is uncorrelated with that at T_2 since the temperature difference ΔT is large so that the domain size $R_{T2}(t_{w2})$ is much larger than $L_{\Delta T}$. The T dependence of χ_{FC} in the FC-2 process is the same as that in the FC-1 process. Note that the

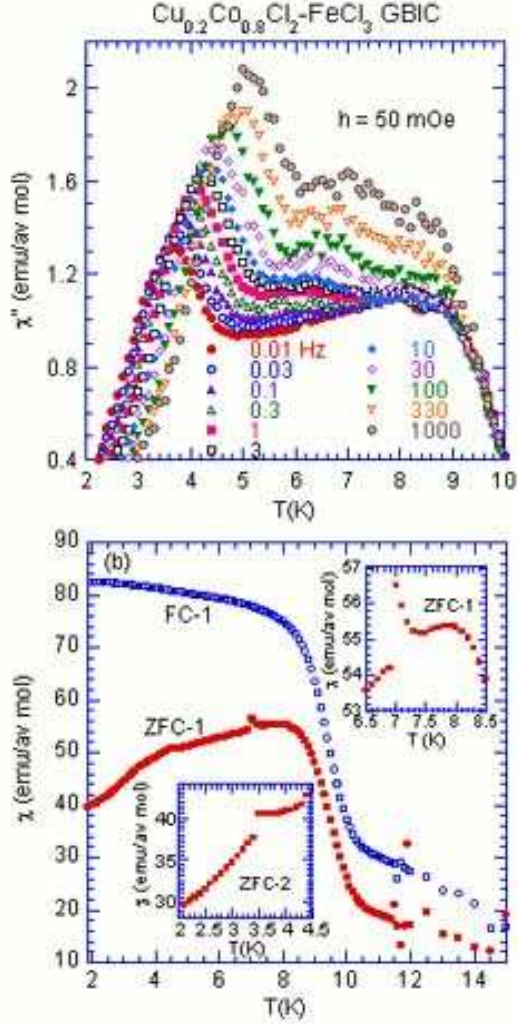


FIG. 2: (Color online)(a) $\chi''(\omega, T)$ vs T at various f ($0.01 \leq f \leq 1000$ Hz). $h = 50$ mOe. (b) T dependence of χ_{ZFC} (●) and χ_{FC} (○) at $H = 1$ Oe for $\text{Cu}_{0.2}\text{Co}_{0.8}\text{Cl}_2\text{-FeCl}_3$ GBIC. The measurement was carried out after the ZFC aging protocol: annealing of the system at 50 K for 1200 sec at $H = 0$ and quenching from 50 to 1.9 K. During the ZFC measurement with increasing T from 1.9 to 20 K, the system was aging at $T_1 = 7.0$ K (ZFC-1 measurement) and $T_2 = 3.5$ K (ZFC-2 measurement) for wait time $t_{w1} = t_{w2} = 1.5 \times 10^4$ sec in the presence of $H = 1$ Oe. After the ZFC measurement, the system was annealed at $T = 50$ K for 1.2×10^3 sec in the presence of $H = 1$ Oe. The FC measurement (denoted as FC-1 and FC-2) was carried with decreasing T from 20 to 1.9 K. The T dependence of FC-1 susceptibility is the same as that of FC-2 susceptibility.

gradual increase of χ_{ZFC} with increasing T from the stop temperature is also observed in the SG phase of the 3D Ising spin glasses $\text{Fe}_{0.5}\text{Mn}_{0.5}\text{TiO}_3$ ³¹ and $\text{Cu}_{0.5}\text{Co}_{0.5}\text{Cl}_2\text{-FeCl}_3$ GBIC.³² Such an aging behavior in χ_{ZFC} may be common to the RSG and SG phases. This is in contrast to the gradual decrease of χ_{ZFC} with increasing T from the stop temperature in the FM phase.

B. T dependence of $S(t)$

We have measure the t dependence of χ_{ZFC} under the condition with various combinations of T , H , and t_w . Figures 3 and 4 show the t dependence of the relaxation rate $S(t)$ at various T ($2.0 \leq T \leq 9.0$ K) for $t_w = 1.5 \times 10^4$ sec and 3.0×10^4 sec, respectively, where $H = 1$ Oe. The relaxation rate $S(t)$ exhibits a broad peak at a characteristic time t_{cr} in the FM phase as well as the RSG phase, indicating the aging behaviors. In Fig. 5 we show the t dependence of χ_{ZFC} at $H = 1$ Oe for $t_w = 3.0 \times 10^4$ sec. We find that $\chi_{ZFC}(t)$ is well described by a stretched exponential relaxation form given by Eq.(15) with $m = 0$ for $10^2 \leq t \leq 3.0 \times 10^4$ sec. The least squares fits of these data to Eq.(15) with $m = 0$ yields the parameters τ , n and A . Figure 6(a) shows the T dependence of t_{cr} and τ for $t_w = 1.5 \times 10^4$ sec, where $H = 1$ Oe. The T dependence of t_{cr} almost agrees well with that of τ for $2 \leq T \leq 9$ K. This indicates that the relaxation is dominated by a stretched exponential relaxation with $m = 0$ (see Sec. IIB). The relaxation time τ ($\approx t_{cr}$) shows a broad peak centered around 5.5 K between T_c and T_{RSG} , and a local minimum around T_{RSG} . It decreases with further increasing T below T_{RSG} . As far as we know, there has been no report on the broad peak of t_{cr} (or τ) in the FM phase of reentrant ferromagnets. The existence of the broad peak around 5.5 K suggests the chaotic nature of the FM phase in our system. The drastic increase of t_{cr} (or τ) below T_{RSG} with decreasing T is a feature common to the SG phases of typical SG systems. Note that at $T = 2$ K no peak in $S(t)$ is observed for $1 \times 10^2 \leq t \leq 6 \times 10^4$ sec. The value of τ is estimated as 7×10^4 sec, which is much larger than t_w . In contrast, as shown in Fig. 6(b) for $t_w = 3.0 \times 10^4$ sec, the value of t_{cr} is larger than that of τ in the FM phase. Both t_{cr} and τ show a broad peak at T between 4 and 5 K. This peak temperature is slightly lower than that for $t_w = 1.5 \times 10^4$ sec, suggesting that the relaxation mechanism is dependent on t_w . In the inset of Fig. 6(a) we show the plot of $1/\tau$ as a function of $1/T$. In the limited temperature range ($2.5 \leq T \leq 3.3$ K), $1/\tau$ can be approximated by an exponential T dependence

$$1/\tau = c_1 \exp(-c_2 T_{RSG}/T), \quad (22)$$

with $c_1 = (1.16 \pm 0.32) \times 10^{-2} \text{ sec}^{-1}$ and $c_2 = 4.2 \pm 0.2$. Our value of c_2 is relatively larger than those derived by Hoogerbeets et al. ($c_2 = 2.5$)^{21,22} from an analysis of thermoremanent magnetization (TRM) relaxation measurements on four SG systems: Ag:Mn (2.6 at. %), Ag:Mn (4.1 at. %), Ag:[Mn (2.6 at. %) + Sb (0.46 at. %)], and Cu:Mn (4.0 at. %). Note that in their work the stretched exponential is taken as representative of the short time ($t < t_w$) relaxation. One must thus be careful in comparing the results.

Figure 7 shows the T dependence of S_{max} (the peak height of $S(t)$ at $t = t_{cr}$) for the following three cases: (i) $H = 1$ Oe and $t_w = 3.0 \times 10^4$ sec, (ii) $H = 1$ Oe and $t_w = 1.5 \times 10^4$ sec, and (iii) $H = 10$ Oe and $t_w = 2.0 \times 10^3$ sec. The peak height S_{max} at $H = 1$ Oe exhibits two

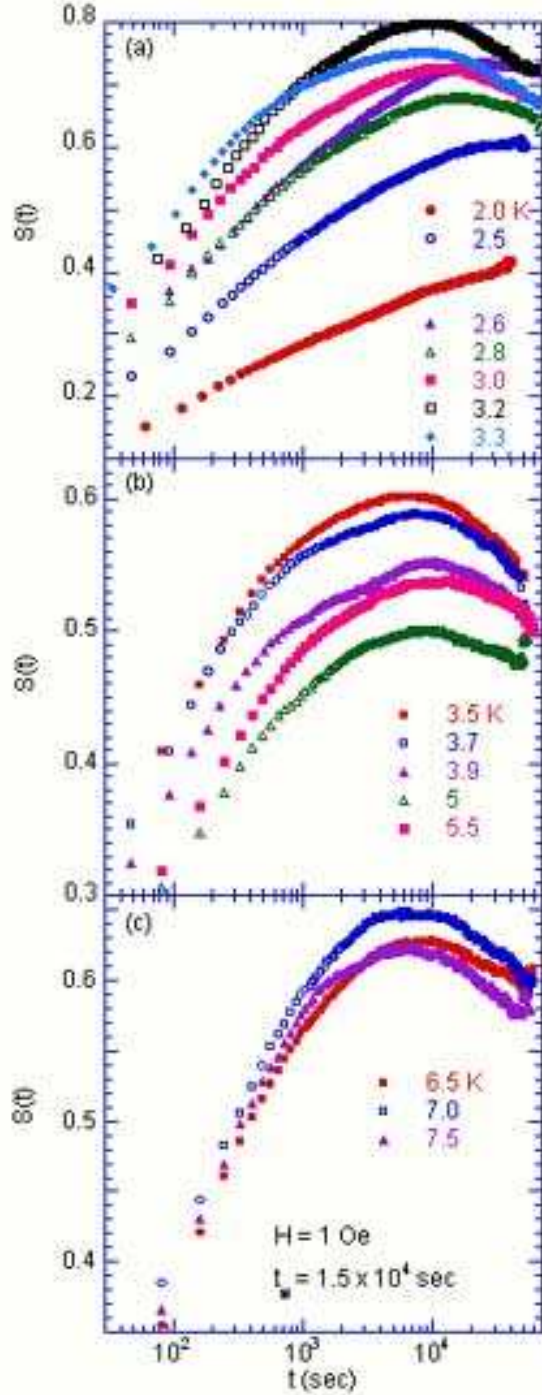


FIG. 3: (Color online)(a) and (b) Relaxation rate $S [= d\chi_{ZFC}/d\ln t]$ vs t at various T . $H = 1$ Oe. $t_w = 1.5 \times 10^4$ sec. H is applied along a direction perpendicular to the c axis. The ZFC aging protocol: annealing of the system at 50 K for 1.2×10^3 sec at $H = 0$, quenching from 50 K to T , and then isothermal aging at T and $H = 0$ for a wait time t_w . The measurement was started at $t = 0$ when the field H is turned on.

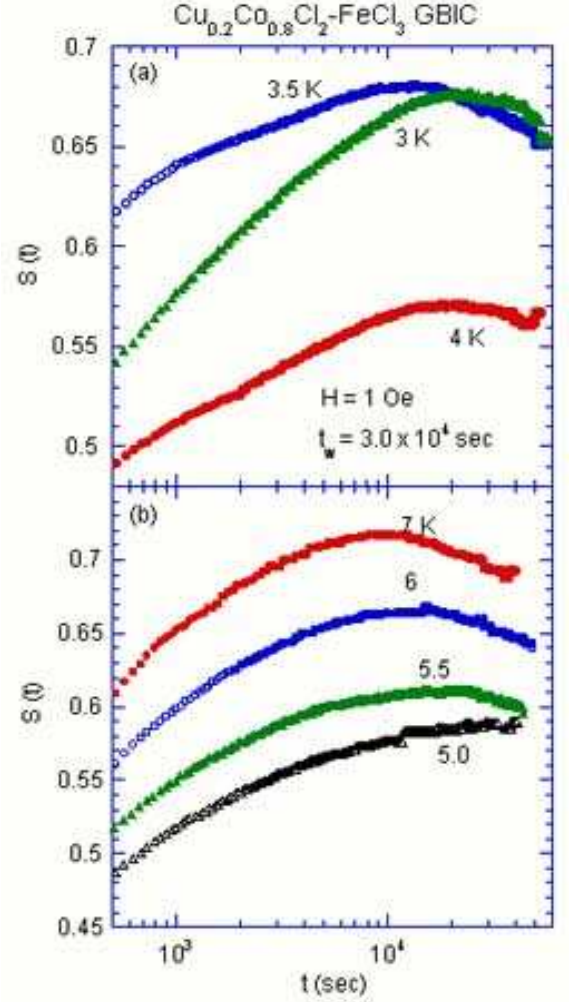


FIG. 4: (Color online)(a) and (b) S vs t at various T . $H = 1$ Oe. $t_w = 3.0 \times 10^4$ sec.

peaks around $T = T_{RSG}$ and at 7.0 K just below T_c , independent of t_w ($= 1.5 \times 10^4$ sec or 3.0×10^4 sec). Note that the peak of S_{max} at 7.0 K is strongly dependent of H : it disappears at $H = 10$ Oe for $t_w = 2.0 \times 10^3$ sec.

In Fig. 8(a) we show the plot of the exponent n as a function of T for $t_w = 1.5 \times 10^4$ and 3.0×10^4 sec, where $H = 1$ Oe. For $t_w = 3.0 \times 10^4$ sec the exponent n increases with increasing T and exhibits a peak at $T = 4$ K just above T_{RSG} . The exponent n decreases with further increasing T , showing a local minimum around 7.5 K. For $t_w = 1.5 \times 10^4$ sec, the exponent n exhibits a local minimum ($n \approx 0.75$) around 2.5 K ($T/T_{RSG} = 2.5/3.5 = 0.71$) and a local maximum ($n \approx 0.79$) around 4.0 K. The local minimum of n below T_{RSG} is a feature common to that of SG systems, where n has a local minimum at $T = T^*$ given by $T^*/T_{SG} \approx 0.70$.^{22,23} The exponent n increases as T approaches T_{SG} from the low- T side. The overall variation of n below T_{SG} is qualitatively the same as that calculated for the Sherrington-Kirkpatrick model.³³

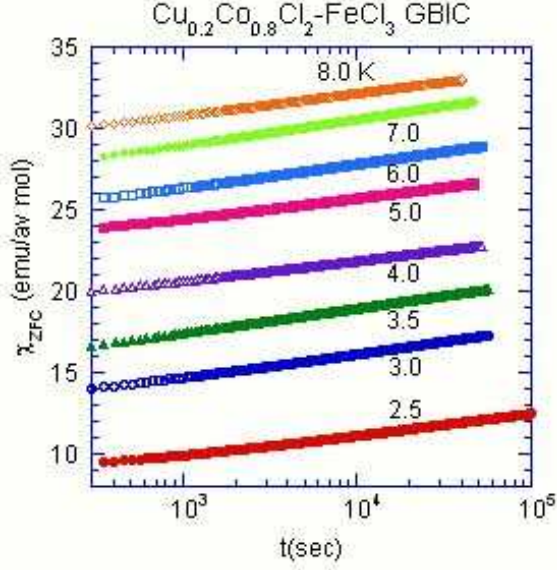


FIG. 5: (Color online) t dependence of $\chi_{ZFC}(t)$ at various T . $H = 1$ Oe. $t_w = 3.0 \times 10^4$ sec. The solid curves are fits to Eq.(15) with $m = 0$ for stretched exponential relaxation.

Figure 8(b) shows the T dependence of the amplitude A for $t_w = 1.5 \times 10^4$ and 3.0×10^4 sec. We find that A is strongly dependent on T . Irrespective of t_w , the amplitude A shows two local maxima at 3 and 7.0 K. For comparison, we evaluate the T dependence of $S_{max}^0 [= A(1-n)/e]$, which corresponds to Eq.(21) with $m = 0$. As the values of n and A , here we use the experimental values at each T shown in Figs. 8(a) and (b). We find that the T dependence of S_{max}^0 thus calculated is in excellent agreement with that of S_{max} (see Fig. 7) experimentally determined from the data of $S(t)$ vs t .

C. $S(t)$ under the H -shift

Figures 9(a) and (b) show the t dependence of $S(t)$ at various H , where $T = 3.3$ and 7.0 K, and $t_w = 1.5 \times 10^4$ sec. The relaxation rate $S(t)$ shows a peak at t_{cr} . This peak greatly shifts to the short- t side with increasing H . In Fig. 10(a) we make a plot of t_{cr} and τ as a function of H at $T = 3.3$ and 7.0 K, where τ is determined from the least squares fit of the data of χ_{ZFC} vs t to the stretched exponential relaxation with $m = 0$. The value of t_{cr} is almost the same as that of τ at each T and H , indicating that the exponent m is equal to zero (see Sec. IIB). The time t_{cr} undergoes a dramatic decrease at low fields: $H \approx 2 - 3$ Oe at $T = 7.0$ K and $H = 10$ Oe at $T = 3.3$ K. Note that the decrease of t_{cr} with H has been reported for the ZFC relaxation in the RSG phase of the reentrant ferromagnet $\text{Fe}_{0.3}\text{Al}_{0.7}$.¹⁰ The increase of n and $1/\tau$ with increasing H has been reported for the TRM decay in the SG systems such as $\text{Ag}:[\text{Mn} (2.6 \text{ at. } \%) + \text{Sb} (0.46 \text{ at. } \%)]$ ²² and $\text{Cu}:\text{Mn} (6 \text{ at. } \%)$.³⁰

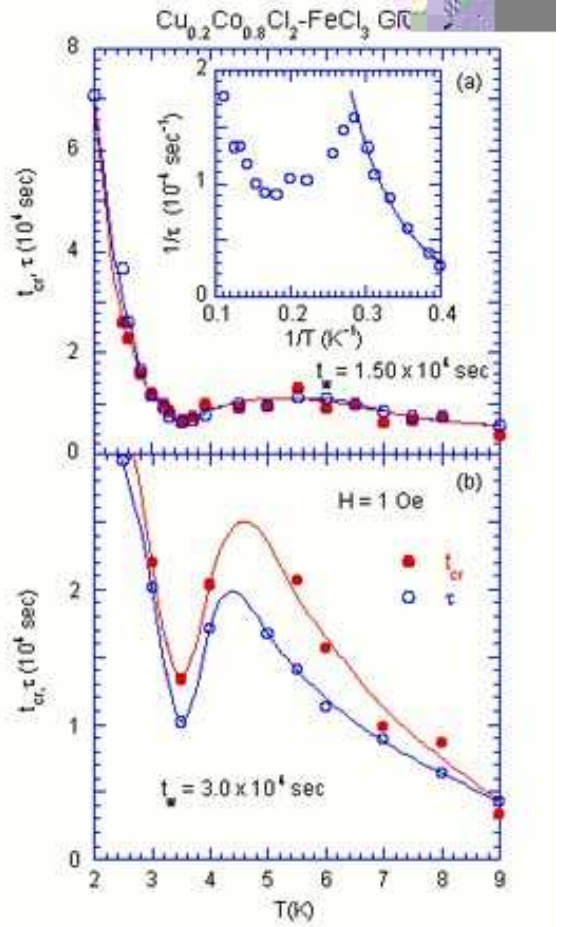


FIG. 6: (Color online) t_{cr} vs T and τ vs T . t_{cr} is a characteristic time at which $S(t)$ has a maximum S_{max} . τ is the relaxation time for the stretched exponential relaxation. $H = 1$ Oe. (a) $t_w = 1.5 \times 10^4$ sec. (b) $t_w = 3.0 \times 10^4$ sec. The solid lines are guide to the eyes. The inset of (a) shows the plot of $1/\tau$ vs $1/T$ ($T < T_{RSG}$), where the solid line is a least-squares fit to Eq.(22). The fitting parameters are given in the text.

The shift of t_{cr} for $S(t)$ under the H -shift process is governed by the mean domain-size $L_T(t)$ and overlap lengths L_H defined by¹³

$$L_T(t)/L_0 \approx (t/t_0)^{1/z(T)} \text{ and } L_H/L_0 \approx (H/\Upsilon_H)^{-1/\delta}, \quad (23)$$

respectively, where $z(T)$ and δ are the corresponding exponents for $L_T(t)$ and L_H , and Υ_H is the magnetic field corresponding to a wall stiffness Υ (a typical energy setting the scale of free energy barriers between conformations). Using the scaling concept, the shift of t_{cr} for $S(t)$ under the H -shift can be approximated by^{32,34}

$$\ln(t_{cr}/t_w) = -\alpha_H H, \quad (24)$$

in the limit of $H \approx 0$, where α_H is constant proportional to $z(T) t_w^{\delta/z(T)}$. In Fig. 10(b) we make a plot of t_{cr} vs H at $T = 3.3$ and 7.0 K. We find that the data of t_{cr} vs H is well described by Eq.(24) with $\alpha_H = 0.128 \pm 0.009$ and

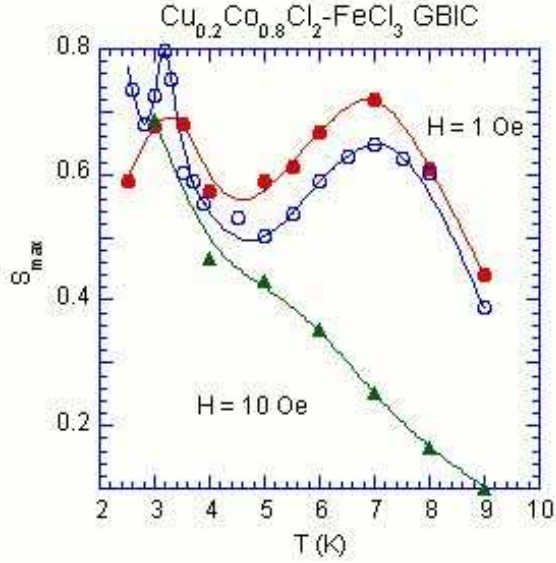


FIG. 7: (Color online) S_{max} vs T for the three cases: (i) $H = 1$ Oe and $t_w = 3.0 \times 10^4$ sec (●), (ii) $H = 1$ Oe and $t_w = 1.5 \times 10^4$ sec (○), and (iii) $H = 10$ Oe and $t_w = 2.0 \times 10^3$ sec (▲). The solid lines are guides to the eyes.

$t_w = (9.19 \pm 0.31) \times 10^3$ sec for $H < 15$ Oe at $T = 3.3$ K and $\alpha_H = 0.63 \pm 0.15$ and $t_w = (12.0 \pm 2.6) \times 10^3$ sec for $H < 1$ Oe at $T = 7.0$ K.

In Fig. 11(a) we show the H dependence of S_{max} at $T = 3.3$ and 7.0 K, where $t_w = 1.5 \times 10^4$ sec. The value of S_{max} is almost independent of H for $0 \leq H \leq 40$ Oe. In contrast, the value of S_{max} at 7.0 K greatly reduces with increasing H . This result agrees well with that reported by Jonason and Nordblad³ with the gradual decrease of S_{max} at 16 K with H and the dramatic decrease in S_{max} at 30 K with H at weak fields less than 0.2 Oe. Figure 11(b) shows the H dependence of the exponent n at $T = 3.3$ and 7.0 K, where $t_w = 1.5 \times 10^4$ sec. The H dependence of n at 7.0 K is rather different from that at 3.3 K at low H . The value of n at $T = 3.3$ K has a local minimum at $H = 5$ Oe, while the value of n at $T = 7.0$ K has a local maximum around 10 Oe. The value of n tends to saturate to $0.82 - 0.84$ at H higher than 30 Oe, independent of T . Figure 11(c) shows the H dependence of A at $T = 3.3$ and 7.0 K, where $t_w = 1.5 \times 10^4$ sec. The amplitude A at 7.0 K deviates from that at 3.3 K above 5 Oe, indicating the fragility of the aging state in the FM phase against a weak magnetic field-perturbation. For comparison, we make a plot of $S_{max}^0 [= A(1 - n)/e]$ as a function of H , where A and n experimentally determined are used. There is a very good agreement between S_{max} (see Fig. 11(a)) and S_{max}^0 .

D. Effect of t_w on $S(t)$

Figure 12 shows the t dependence of $S(t)$ at various t_w for $T = 3.5$ and 7.0 K, where $H = 1$ Oe. The relax-

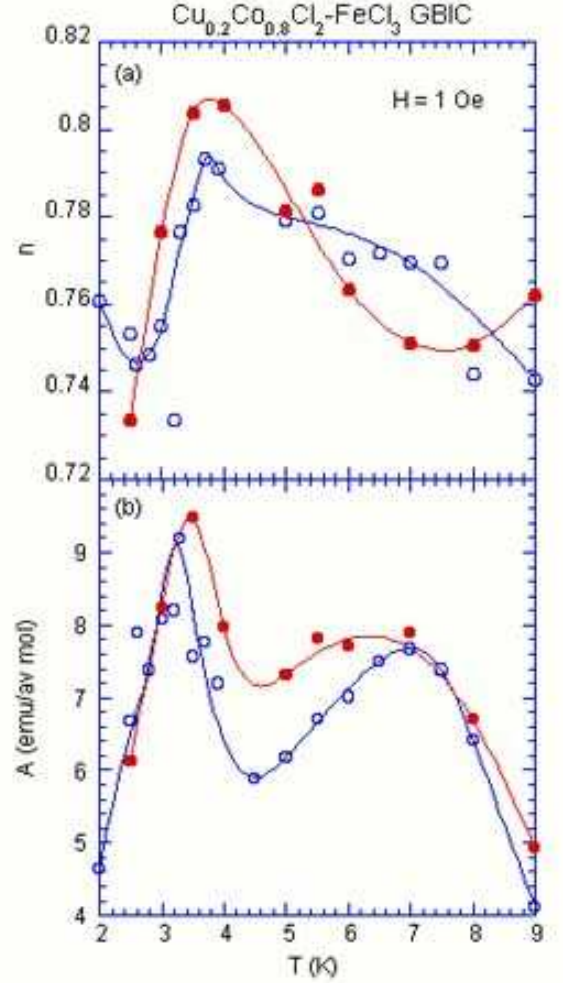


FIG. 8: (Color online)(a) n vs T and (b) A vs T , where $t_w = 3.0 \times 10^4$ sec (●) and 1.5×10^4 sec (○). $H = 1$ Oe. The solid lines are guides to the eyes.

ation rate $S(t)$ shows a peak at t_{cr} . This peak shifts to long- t side with increasing t_w . The least squares fit of the data of $\chi_{ZFC}(t)$ vs t for $1.0 \times 10^2 \leq t \leq 6.0 \times 10^4$ sec to Eq.(15) yields the exponent n , the relaxation time τ , and amplitude A for the stretched exponential relaxation. Figure 13(a) shows the t_w dependence of t_{cr} and τ at $T = 3.5$ and 7.0 K. At $T = 7.0$ K, t_{cr} is nearly equal to τ for $0 < t_w \leq 3.0 \times 10^4$ sec, while at $T = 3.5$ K t_{cr} is much longer than τ for $t_w \geq 1.5 \times 10^4$ sec. Both t_{cr} and τ increases with increasing t_w . It has been reported that τ varies exponentially with t_w as $\tau = \tau_0 \exp(t_w/t_0)$ for Ag: Mn (2.6 at. %).²² Our data of τ vs t_w at 3.5 K are well fitted to this equation in spite of the limited t_w region ($1.0 \times 10^4 \leq t_w \leq 3.0 \times 10^4$ sec); $\tau_0 = (3.83 \pm 0.012) \times 10^3$ sec and $t_0 = (3.07 \pm 0.13) \times 10^4$ sec. Figure 13(b) shows the t_w dependence of n at $T = 3.5$ and 7.0 K. The exponent n at $T = 3.5$ K shows a local minimum at $t_w = 1.0 \times 10^4$ sec and increases with further increasing t_w . In contrast, the exponent n at 7.0 K is smaller than that at 3.5 K for any t_w . It exhibits a local maximum

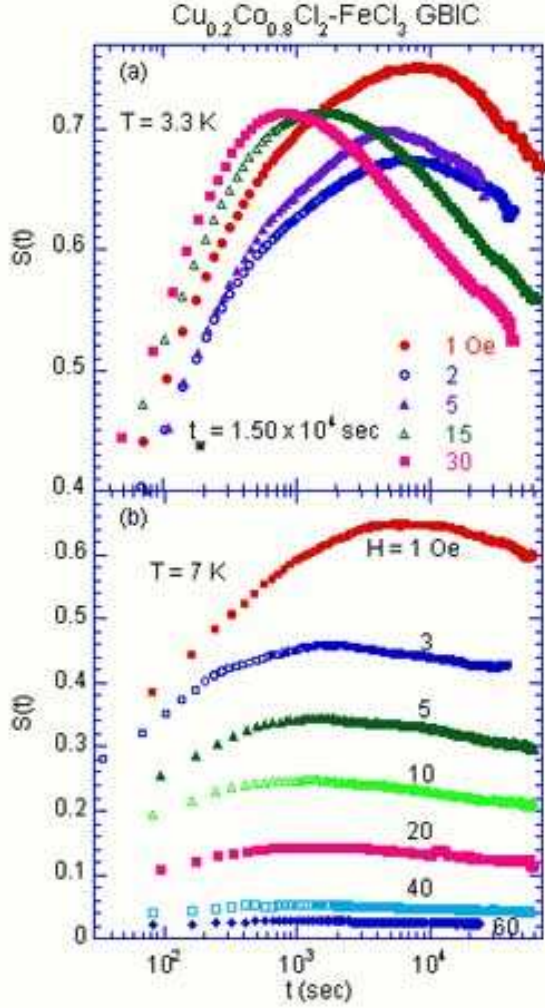


FIG. 9: (Color online) S vs t at various H . (a) $T = 3.3$ K and $t_w = 1.5 \times 10^4$ sec. (b) $T = 7.0$ K and $t_w = 1.5 \times 10^4$ sec.

around $t_w = 5.0 \times 10^3$ sec. Similar local minimum in n vs t_w is observed in the SG phase of the spin glass $\text{Cr}_{83}\text{Fe}_{17}$ [$T_{SG} = 13$ K]:⁵ n at $T = 8$ K shows a local minimum around $t_w = 3.0 \times 10^3$ sec and increases with further increasing t_w . In contrast, there is no local minimum in n vs t_w in the RSG phase of $(\text{Fe}_{0.65}\text{Ni}_{0.35})_{0.882}\text{Mn}_{0.118}$ ⁶ (n increases with increasing t_w) and in the SG phase of Ag: Mn (2.6 and 4.1 at. %)²² (n is independent of t_w). Figure 13(c) shows the t_w dependence of the amplitude A at $T = 3.5$ and 7.0 K. The amplitude A at 3.5 K shows a local minimum around $t_w = 1.0 \times 10^4$ sec, while A at 7.0 K is almost independent of t_w . In summary, so far there has been no theory to explain the t_w dependence of n , τ , t_{cr} and A in both the RSG and FM phases. However, our results suggest that the RSG and FM phases are essentially nonequilibrium phases. The nature of the aging behavior in the FM phase is rather different from that in the RSG phase.

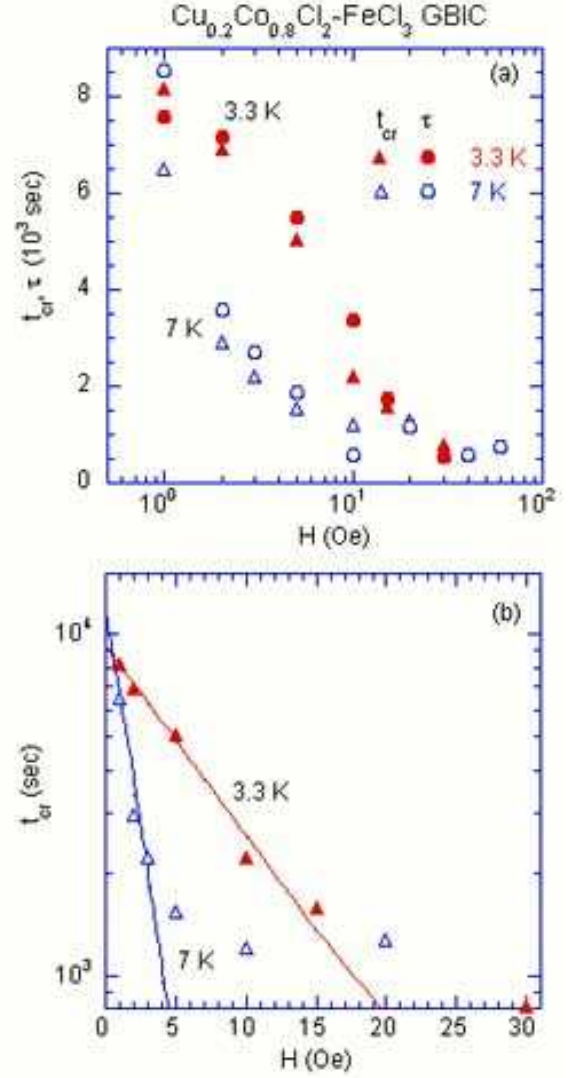


FIG. 10: (Color online)(a) t_{cr} vs H and τ vs H at $T = 3.3$ and 7.0 K. The solid lines are guides to the eyes. (a) t_{cr} vs H at $T = 3.3$ and 7.0 K. The solid lines are least-squares fits to Eq.(24) for data at low H . The fitting parameters are given in the text.

E. $S(t)$ under the T -shift

Figure 14(a) show the relaxation rate $S(t)$ measured at $T_f = 7.0$ K for different initial temperature T_i ($= 4.9, 5.6,$ and 6.3 K), where $t_w = 3.0 \times 10^4$ sec and $H = 1$ Oe. The measurement was carried out as follows. After the ZFC protocol from 50 K to T_i below T_c , the system was kept at T_i for a wait time t_w . Immediately after T was changed from T_i to T_f (the positive T shift; $\Delta T > 0$ where $\Delta T = T_f - T_i$), the magnetic field was applied and the t dependence of χ_{ZFC} was measured.

With increasing ΔT , the time t_{cr} shifts to the low- t side. The relaxation rate $S(t)$ has a peak at $t_{cr} = 440 - 460$ sec at $\Delta T = 2.1$ K and 1.4 K, suggesting a rejuvene-

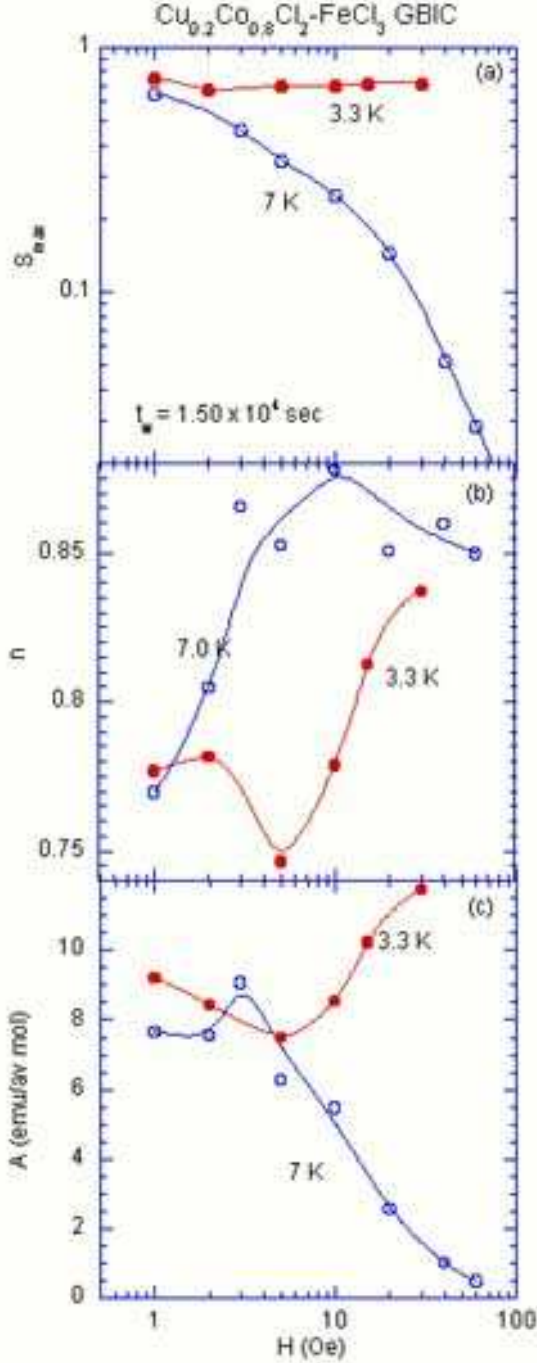


FIG. 11: (Color online)(a) S_{max} vs H , (b) n vs H , and (c) A vs H at $T = 3.3$ and 7.0 K. $t_w = 1.5 \times 10^4$ sec. $H = 1$ Oe. The solid lines are guides to the eyes.

nation of the system during the positive T -shift. For $\Delta T = 0.7$ K two peaks appear at 570 sec and 1210 sec, respectively, suggesting a coexistence of two characteristic ages in the system due to the partial rejuvenation and original aging at T_i for $t_w = 3.0 \times 10^4$ sec. This behavior is explained in terms of the overlap length $L_{\Delta T}$, which becomes smaller as ΔT becomes

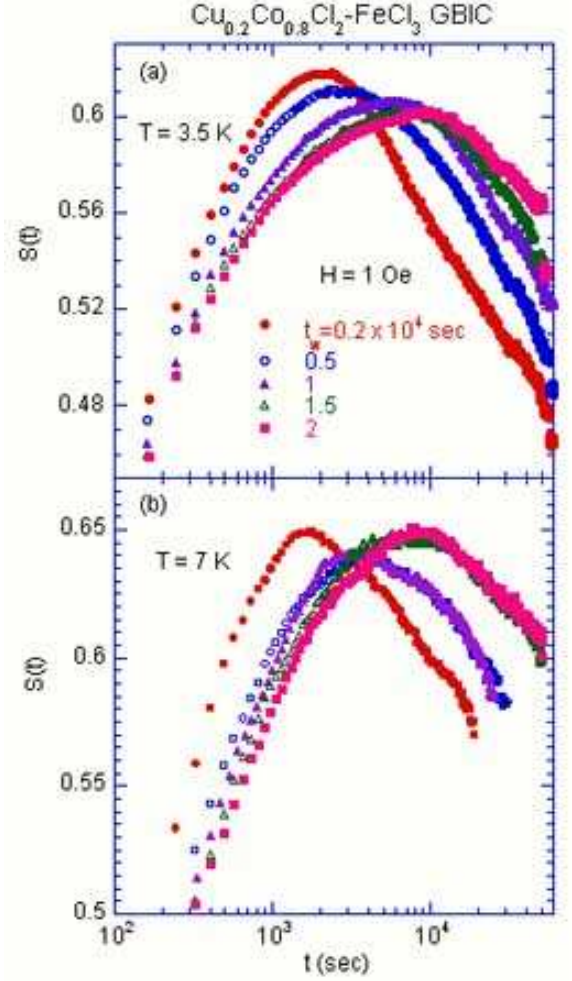


FIG. 12: (Color online) S vs t at various t_w ($2 \times 10^3 \leq t_w \leq 3.0 \times 10^4$ sec). $H = 1$ Oe. (a) $T = 3.5$ K. (b) $T = 7.0$ K.

large. When $R_{Ti}(t_w) \ll L_{\Delta T}$ corresponding to the case of $\Delta T < \Delta T_{threshold}$, no initialization occurs in the system. There is only one type of domain. Thus $S(t)$ exhibits a peak around t_w . For $R_{Ti}(t_w) \gg L_{\Delta T}$ corresponding to the case of $\Delta T > \Delta T_{threshold}$, some domains fractures into smaller domains of dimension $L_{\Delta T}$. Thus $S(t)$ has two peaks at t_{cr} ($\approx t_w$) and a time much shorter than t_{cr} .

The shift of t_{cr} for $S(t)$ under the T -shift aging process is governed by the mean domain-size $L_T(t)$ and overlap length $L_{\Delta T}$ defined by¹³

$$L_{\Delta T}/L_0 \approx (T^{1/2} |\Delta T| / \Upsilon_T^{3/2})^{-1/\zeta}, \quad (25)$$

where ζ is the corresponding exponent and Υ_T is the temperature corresponding to the wall stiffness Υ . Using the scaling concepts, the shift of t_{cr} for $S(t)$ under the T -shift can be approximated by^{32,35,36}

$$\ln(t_{cr}/t_w) = -\alpha_T |\Delta T|, \quad (26)$$

in the limit of $H \approx 0$, where α_T is a constant proportional

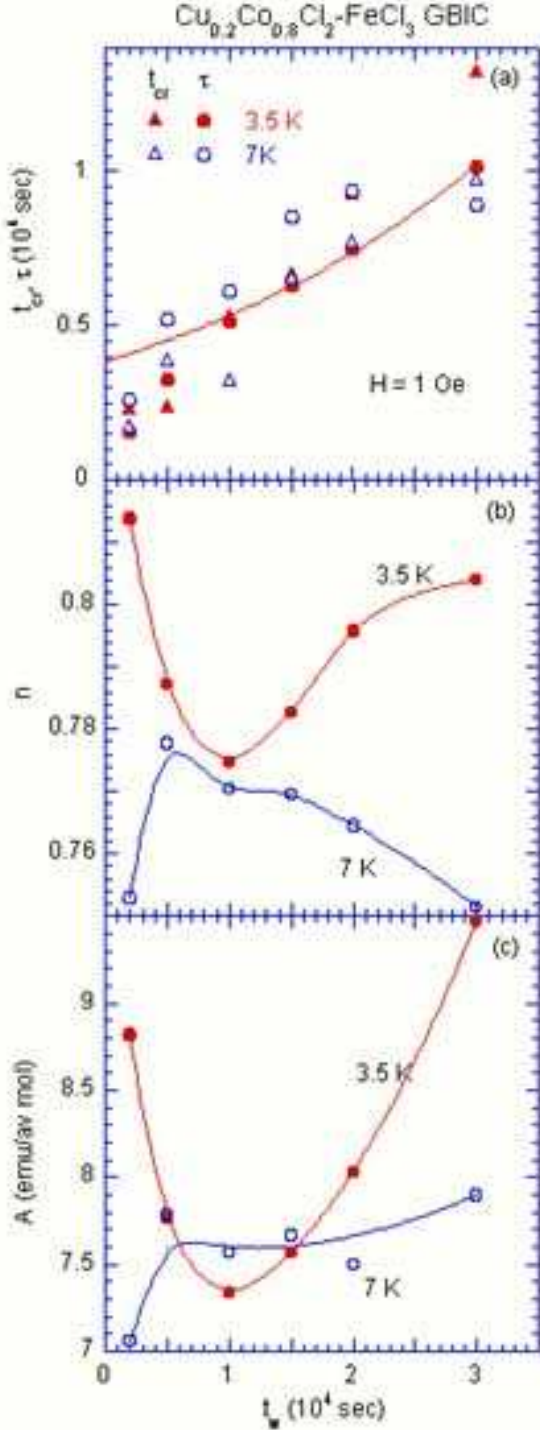


FIG. 13: (Color online)(a) t_{cr} vs t_w and τ vs t_w . The solid line is a least-squares fit to $\tau = \tau_0 \exp(t_w/t_0)$ for τ at 3.5 K ($t_w \geq 1.0 \times 10^4$ sec). The fitting parameters are given in the text. (b) n vs t_w , and (c) A vs t_w at $T = 3.5$ and 7.0 K. The solid lines are guides to the eyes.

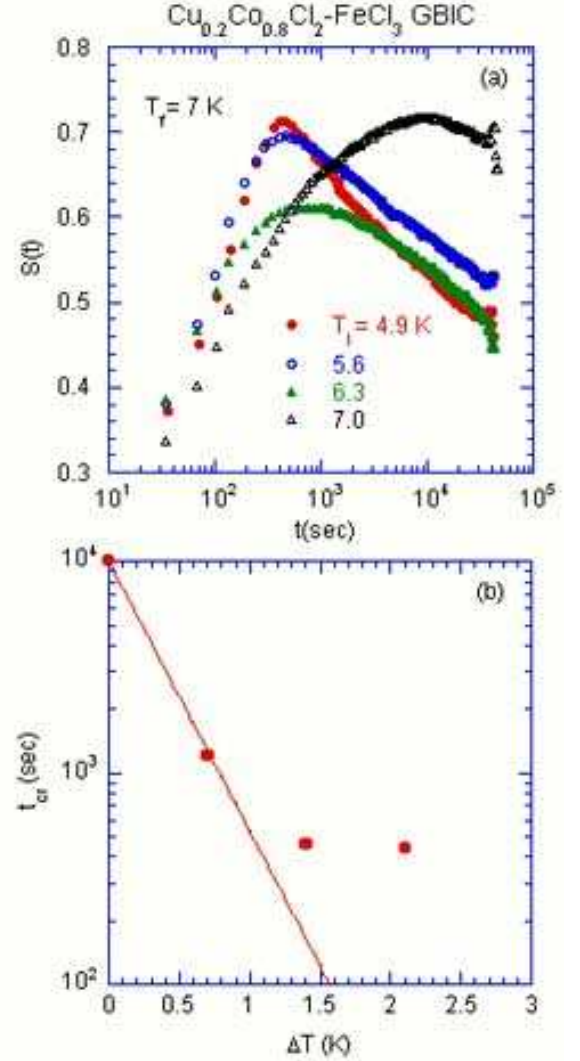


FIG. 14: (Color online)(a) t dependence of S at $T = T_f = 7.0$ K under the T shift from T_i to T_f , where $T_i = 4.9, 5.6$, and 6.3 K. $H = 1$ Oe. The ZFC aging protocol is as follows: quenching of the system from 50 K to T_i , and isothermal aging at $T = T_i$ and $H = 0$ for $t_w = 3.0 \times 10^4$ sec. The measurement was started at $t = 0$, just after T was shifted from T_i to T_f and subsequently H ($= 1$ Oe) was turned on. (b) t_{cr} vs ΔT . The solid line is a fitting curve to Eq.(26). The fitting parameters are given in the text.

to $z(T_f)T_f^{1/2}t_w^{z(T_i)}$. In Fig. 14(b) we make a plot of t_{cr} vs ΔT at $T_f = 7.0$ K. We find that the data of t_{cr} vs ΔT is described by Eq.(26) with $\alpha_T = 2.93 \pm 0.33$ and $t_w = (10.0 \pm 0.3) \times 10^3$ sec for $\Delta T < 0.7$ K.

Similar behaviors in $S(t)$ under the T shift have been observed in other reentrant ferromagnets. In the FM phase of $(\text{Fe}_{0.20}\text{Ni}_{0.80})_{75}\text{P}_{16}\text{B}_6\text{Al}_3$,^{1,4} the amplitude of the maximum in $S(t)$ at $t \approx t_w$ decreases with increasing $|\Delta T|$ (both the positive and negative T -shift) and a second maximum gradually develops at a shorter time, indicating a partial rejuvenation. In the RSG phase of

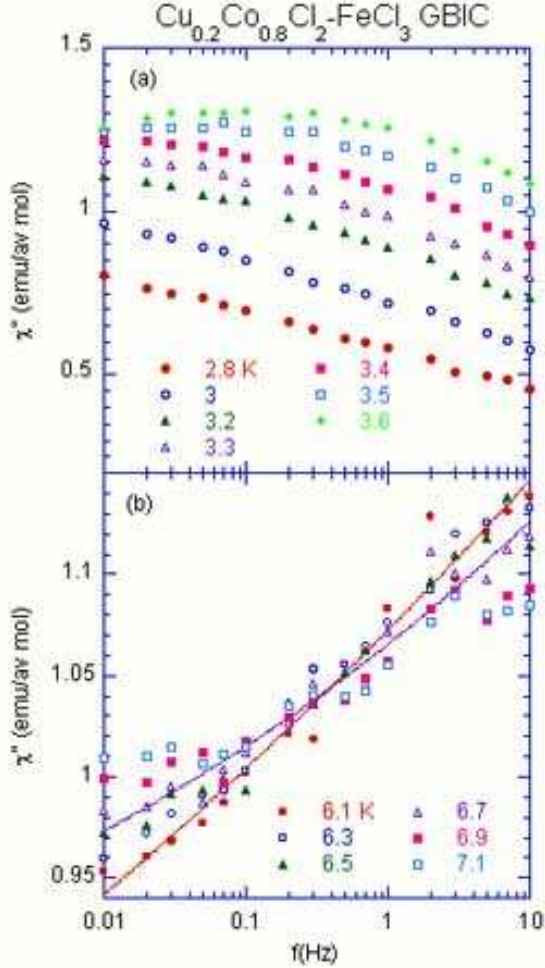


FIG. 15: (Color online)(a) and (b) f dependence of $\chi''(\omega, T)$ at various T . $h = 50$ mOe. The solid lines are least-squares fits to Eq.(14) for $T = 6.1$ and 6.7 K. The fitting parameters are given in the text.

$(\text{Fe}_{0.65}\text{Ni}_{0.35})_{0.882}\text{Mn}_{0.118}$ double peaks in $S(t)$ vs t are observed under a temperature-cycling experiment:⁶ an initial wait time t_w ($= 1.0 \times 10^4$ sec) at T , followed by a temperature cycle $T \rightarrow T + \Delta T \rightarrow T$ of the duration t_{cycle} ($= 300$ sec).

F. $\chi''(\omega, t)$

In previous paper¹¹ we have reported the f dependence of the equilibrium absorption $\chi''(\omega, T)$ at various T in the vicinity of T_{RSG} , respectively. The absorption $\chi''(\omega, T)$ curves exhibit different characteristics depending on T . Above T_{RSG} , $\chi''(\omega, T)$ shows a peak at a characteristic frequency, shifting to the low f -side as T decreases. Below T_{RSG} , $\chi''(\omega, T)$ shows no peak for $f \geq 0.01$ Hz. In Figs. 15 (a) and (b), for comparison we show the f dependence of $\chi''(\omega, T)$ at fixed T ($2.8 \leq T \leq 3.6$ K and $6.1 \leq T \leq 7.1$ K). The absorp-

TABLE I: Exponents α (or b) determined from the least squares fits of $\chi''(\omega, t)$ at f to the power law form by given by Eq.(27). $T = 3.5, 3.75, 7$ and 8.5 K. The parameters with the suffix “c” denote those determined from the least squares fits of the data to a power-law form $(t + t_0)^{-b}$ instead of t^{-b} , where t_0 is regarded as a fitting parameter.

T (K)	f (Hz)	$\alpha(b)$	A	$\chi''_0(\omega)$
3.5	0.1	0.070	0.182	1.100
3.75	0.05	0.084	0.137	1.228
7	0.05	0.074	0.334	0.662
7	0.1	0.045	0.458	0.537
7	0.5	0.042	0.386	0.606
7	1	0.029	0.505	0.489
7	5	0.015	0.770	0.265
7 ^c	0.05	0.224	0.216	0.822
7 ^c	0.1	0.072	0.324	0.676
7 ^c	0.5	0.069	0.267	0.729
7 ^c	1	0.047	0.333	0.665
8.5	0.05	0.147	0.148	0.835
8.5	1	0.046	0.268	0.702

tion $\chi''(\omega, T)$ decreases with increasing f in the RSG phase, while it increases with increasing f in the FM phase. The f dependence of $\chi''_{\text{eq}}(\omega, T)$ can be expressed by a power law form ($\approx \omega^\alpha$), where the magnitude of the exponent α is very small. The sign of α may be negative for the RSG phase and is positive for the FM phase. According to the fluctuation-dissipation theorem, the magnetic fluctuation spectrum $P(\omega, T)$ is related to $\chi''_{\text{eq}}(\omega, T)$ by $P(\omega, T) = 2k_B T \chi''_{\text{eq}}(\omega, T)/\omega$. Then $P(\omega, T)$ is proportional to $\omega^{-1+\alpha}$, which is similar to $1/\omega$ character of typical SG systems. Note that for the spin glass $\text{CdCr}_{1.7}\text{In}_{0.3}\text{S}_4$ ($T_{\text{SG}} = 16.7$ K),³⁷ α (≈ 0.1) is positive at T_{SG} and decreases with decreasing T . The sign of α changes from positive to negative below 5 K: $\alpha \approx -0.03$.

In contrast, $\chi''(\omega, T)$ for $6.0 \leq T \leq 7.4$ K increases with increasing f . The least squares fit of the data of $\chi''(\omega, T)$ vs f for $0.01 \leq f \leq 10$ Hz to the power law form ($\approx \omega^\alpha$) yields the value of α . The exponent α increase with increasing T for $6.1 \leq T \leq 7.2$ K: $\alpha = 0.04 \pm 0.01$ at 6.1 K, 0.081 ± 0.02 at 6.7 K and $\alpha = 0.12 \pm 0.02$ at 7.2 K.

We have also measured the t dependence of $\chi''(\omega, t)$ at $T = 3.3, 3.5, 3.75, 7$ and 8.5 K, where $H = 0$, $h = 0.3$ Oe, and $f = 0.05 - 5$ Hz. The system was quenched from 100 K to T at time (age) zero. The origin $t = 0$ is a time at which the temperature becomes stable at T within ± 0.01 K. The change of $\chi''(\omega, t)$ with t below T_{RSG} is not so prominent compared to that above T_{RSG} , partly because of relatively small magnitude of χ'' below T_{RSG} . In Figs. 16(a)-(c), we shows the t dependence of $\chi''(\omega, t)$ at various f , where $T = 3.75, 7.0$, and 8.5 K. We find that the decrease of χ'' with increasing t is well described by

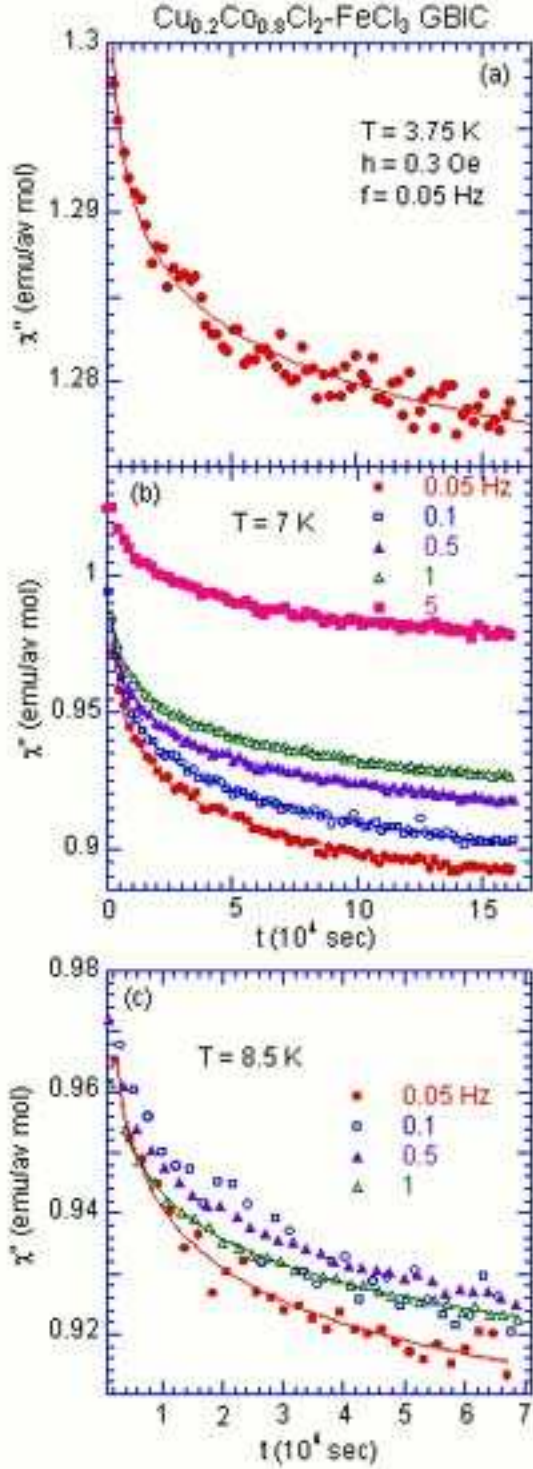


FIG. 16: (Color online) t dependence of $\chi''(\omega, t)$ at (a) 3.75 K, (b) $T = 7.0$ K, and (c) $T = 8.5$ K. $f = 0.05, 0.1, 0.5$ and 1 Hz. The time t is the time taken after the sample is quenched from 50 K to T . $H = 0$. The solid lines are the least-squares fits to Eq.(27). The fitting parameters are listed in Table I.

a power-law decay of the quasi-equilibrium part

$$\chi''(\omega, t) \approx \chi''_{eq}(t) = \chi''_0(\omega) + A(\omega)t^{-\alpha} \quad (27)$$

where $\chi''_0(\omega)$ and $A(\omega)$ are t -independent constants. It is predicted that $\chi''_{eq}(t)$ exhibits no ωt -scaling law [$\chi''_{eq}(t) \approx t^{-\alpha}$]. In the limit of $t \rightarrow \infty$, $\chi''(\omega, t)$ tends to $\chi''_0(\omega)$ which is assumed to be equal to $\chi''(\omega, T)$. The least squares fit of the data of $\chi''(\omega, t)$ at each T to Eq.(27) yields parameters listed in Table I at $T = 3.5, 3.75, 7$, and 8.5 K. The exponent α below T_{RSG} is nearly equal to $0.07 - 0.084$. At 7.0 K, the exponent α is dependent on f : $\alpha = 0.074$ at $f = 0.05$ Hz and $\alpha = 0.015$ at $f = 5$ Hz. The value of χ''_0 at $T = 7.0$ K tends to decrease with increasing f . This seems to be inconsistent with our result that χ''_{eq} increases with increasing f . Since the value of A tends to increase with increasing f , it follows that the second term of Eq.(27) does not obey the ωt -scaling law as is predicted.

In general, $\chi''(\omega, t)$ consists of the quasi-equilibrium part $\chi''_{eq}(t)$ and the aging relaxation part $\chi''_{ag}(\omega t)$. The aging part $\chi''_{ag}(\omega t)$ is predicted to be described by a ωt -scaling law [$\chi''_{ag}(\omega t) \approx (\omega t)^{-b}$].¹⁵ Note that the ωt -scaling of $\chi''(\omega, t)$ is observed in the RSG phase ($T = 8$ K) and the FM phase ($T = 40$ K) of the reentrant ferromagnet $\text{CdCr}_{1.9}\text{In}_{0.1}\text{S}_4$ ($T_{RSG} = 18$ K and $T_c = 50$ K).⁷ The absorption $\chi''(\omega, t)$ mainly arises from $\chi''_{ag}(\omega t)$ but not from $\chi''_{eq}(t)$. The aging relaxation part $\chi''_{ag}(\omega, t)$ is assumed to be described by the power-law form $[\omega(t + t_0)]^{-b}$, instead of $(\omega t)^{-b}$, where $b = 0.2$ for both temperatures and t_0 is an off-set time which takes into account the fact that the cooling procedure is not instantaneous. The least squares fit of our data of $\chi''(\omega, t)$ vs t at $T = 7.0$ K to the power-law form $A(t + t_0)^{-b}$ yields the parameters listed in Table I, where t_0 is one of the fitting parameters. We find that the value of b for $f = 0.05$ Hz ($b = 0.22 \pm 0.06$) is close to that for $\text{CdCr}_{1.9}\text{In}_{0.1}\text{S}_4$.⁷ However, the value of b for higher f is still on the order of $0.047 - 0.07$, which is much smaller than 0.2 . This result indicates that $\chi''(\omega, t) \approx \chi'_{eq}(t) \approx t^{-\alpha}$ in our system.

V. DISCUSSION

A. Dynamic nature of the RSG and FM phases

The nature of the RSG and FM phases for $\text{Cu}_{0.2}\text{Co}_{0.8}\text{Cl}_2\text{-FeCl}_3$ GBIC is summarized as follows. The static and dynamic behavior of the RSG phase is characterized by that of the normal SG phase: a critical exponent $\beta = 0.57 \pm 0.10$ for the SG parameter and a dynamic critical exponent $x = 8.5 \pm 1.8$ for the characteristic relaxation time.¹¹ The aging phenomena are clearly seen in the RSG phase, although no appreciable nonlinear magnetic susceptibility is observed. The exponent n for the stretched exponential relaxation exhibits a local minimum just below T_{RSG} , and increases when T approaches T_{RSG} from the low- T side. The relaxation time

τ for the stretched exponential relaxation drastically increases with decreasing T below T_{RSG} . In this sense, it follows that the RSG phase below T_{RSG} is a normal SG phase.

In contrast, the dynamic nature of the FM phase is rather different from that of an ordinary ferromagnet. A prominent nonlinear susceptibility is observed between T_{RSG} and T_c .¹¹ Aging phenomena and a partial rejuvenation effect under the T -shift are also seen in the FM phase. This aging state disappears even in a weak magnetic field ($H > H_0$; $H_0 = 2 - 5$ Oe). The relaxation time τ (or $t_{cr} \approx \tau$) as a function of T exhibits a local maximum between T_{RSG} and T_c . These results suggest that no long range ferromagnetic correlation exist in the RSG phase. The chaotic behavior of the FM phase is rather similar to that observed in the RSG phase.

Similar behaviors have been observed in the reentrant ferromagnets. In $(\text{Fe}_{0.20}\text{Ni}_{0.80})_{75}\text{P}_{16}\text{B}_6\text{Al}_3$,^{1,2,3,4} the relaxation time diverges at a finite temperature ($\approx T_{RSG}$) with a dynamic critical exponent similar to that observed for normal SG transitions. The FM phase just above T_{RSG} shows a dynamic behavior characterized by an aging effect and chaotic nature similar to that of RSG phase. In $\text{CdCr}_{2x}\text{In}_{2(1-x)}\text{S}_4$ with $x = 0.90, 0.95$, and 1.0 ,^{7,8} the aging behavior of the low frequency AC susceptibility is observed both in the FM and RSG phases, with the same qualitative features as in normal SG systems.

In the mean-field picture,^{33,38,39,40} a true reentrance from the FM phase to the normal SG phase is not predicted. There exists a normal FM long range order in the FM phase. This picture, which assumes infinite-range interactions, is not always appropriate for real reentrant magnets where the short-range interactions are large and random in sign and the spin symmetry is rather Heisenberg-like than Ising-like. In a picture proposed by Aeppli et al.⁴¹, the system in the FM phase consists of regions which by themselves would order ferromagnetically and other regions forming paramagnetic (PM) clusters. The frustrated spins in the PM clusters can generate random molecular fields which act on the unfrustrated spins in the infinite FM network. In the FM phase well above T_{RSG} , the fluctuations of the spins in the PM clusters are so rapid that the FM network is less influenced by them and their effect is only to reduce the net FM moment. On decreasing the temperature toward T_{RSG} , the thermal fluctuations of the spins in the PM clusters become slower. The coupling between the PM clusters and the FM network becomes important and the molecular field from the slow PM spins acts as a random magnetic field. This causes a breakup of the FM network into finite-sized clusters. Below T_{RSG} , the ferromagnetism completely disappears, leading to a RSG phase.

B. Comparison with $S(t)$ in other reentrant ferromagnets

We have shown that the t dependence of $S(t)$ is strongly dependent on T , H , and t_w . Here we compare our results on $S(t)$ with those observed in other reentrant ferromagnets. In order to facilitate the comparison, we have determined the time t_{cr} and the peak height S_{max} from their original data of S vs t . The first case is the results of $S(t)$ for $(\text{Fe}_{0.20}\text{Ni}_{0.80})_{75}\text{P}_{16}\text{B}_6\text{Al}_3$ ($T_{RSG} = 14.7$ K and $T_c = 92$ K) reported by Jonason and Nordblad.³ They have shown that $S(t)$ exhibits a peak at t_{cr} in both RSG and FM phases, indicating that the aging phenomena occur in both phases. These results are in good agreement with our results [see Figs. 3 and 4]. The aging state in the FM phase is fragile against a very weak magnetic-field perturbation. There is a threshold magnetic field H_0 , below which there is a linear response of the relaxation. The field H_0 undergoes a dramatic decrease with increasing T above T_{RSG} . The value of H_0 (≈ 0.5 Oe) for $T < T_{RSG}$ is much lower than that for our system ($H_0 \approx 2 - 5$ Oe). The time t_{cr} decreases with increasing T at low T , showing a local minimum around 23 K, and increases with increasing T between 25 and 30 K. Although there have been no data on $S(t)$ above 30 K, it is assumed that t_{cr} shows a local maximum between 30 K and T_c , since t_{cr} should reduce to zero above T_c . Such a possible local maximum is similar to a local maximum of t_{cr} in the RSG phase observed in our system [see Figs. 6(a) and (b)]. Here we discuss the T dependence of the peak height S_{max} . The peak height S_{max} ($H = 0.5$ Oe and $t_w = 1.0 \times 10^3$ sec) exhibits a peak at 13 K just below T_{RSG} , having a local minimum at 25 K, and tends to increase with further increasing T . Although there have been no data on $S(t)$ above 30 K, it is assumed that S_{max} shows a local maximum between 30 K and T_c , since S_{max} should reduce to zero above T_c . These two peaks of S_{max} vs T are similar to two local maxima around T_{RSG} and between T_{RSG} and T_c in our system. Next we discuss the H dependence of the peak height S_{max} . The peak height S_{max} ($t_w = 1.0 \times 10^3$ sec) decreases with increasing H at both $T = 16$ and 30 K. The drastic decrease of S_{max} at $T = 30$ K occurs even at $H = 0.2$ Oe, while the decrease of S_{max} at 16 K with H is much weaker at low H below 1 Oe. The H -dependence of S_{max} at 16 and 30 K is similar to that at $T = 3.3$ and 7.0 K for our system (see Fig. 11(a)).

The second case is the results of $S(t)$ for $\text{Fe}_{0.70}\text{Al}_{0.30}$ ($T_{RSG} = 92$ K and $T_c = 400$ K). Motoya et al.¹⁰ have reported the t dependence of $S(t)$ at various T only in the RSG phase, where $H = 10$ Oe and $t_w = 3.6 \times 10^3$ sec. The relaxation rate $S(t)$ shows a peak at t_{cr} . The time t_{cr} decreases with increasing T below T_{RSG} , while the peak height S_{max} exhibits a peak at 50 K well below T_{RSG} . These results are in good agreement with our results: see Figs. 6(a) and (b) for $t_{cr}(T)$ and Fig. 7 for $S_{max}(T)$ having a local maximum in S_{max} at 3.2 K below T_{RSG} . Motoya et al.¹⁰ have also measured the t dependence of

$S(t)$ at 10 K at various H , where $T = 10$ K and $t_w = 3.6 \times 10^3$ sec. Both t_{cr} and S_{max} decrease with increasing H . This result is in good agreement with our results: see Fig. 10(a) for $t_{cr}(H)$ and Fig. 11(a) for $S_{max}(H)$.

C. Scaling of $\chi_{ZFC}(t)$ and $\chi''(\omega, t)$

As is described in Sec. II A, the t dependence of $\chi_{ZFC}(t)$ and $\chi''(\omega, t)$ arises from that of the spin autocorrelation function $C(t_w; t + t_w)$ and $C(\Delta t_w; t + \Delta t_w)$, respectively, where $\Delta t_w = 2\pi/\omega$. Here we assume that $C(t_w; t + t_w)$ is defined by either Eqs.(5) or (6). The function $C_{ag}(t_w; t + t_w)$ is approximated by a scaling function $F(t/t_w)$, where $F(x)$ has a power-law form x^{-b} for $x \gg 1$. In the present work, t_w takes various values as $\Delta t_w = 1/f = 10^{-3} - 100$ sec ($0.01 \leq f \leq 1000$ Hz) for $\chi''(\omega, t)$ and as a wait time $t_w = (0.2 - 3.0) \times 10^4$ sec for $\chi_{ZFC}(t)$. The function $C_{eq}(t)$ is independent of t_w and is expressed by a power-law form ($\approx t^{-\alpha}$) given by Eq.(7). By the appropriate choice of t and t_w (or Δt_w), it is experimentally possible to separate the quasi-equilibrium part $C_{eq}(t)$ and the aging part $C_{ag}(t_w; t + t_w)$. Our experimental results are as follows. (i) The absorption $\chi''(\omega, t)$ mainly comes from the quasi-equilibrium contribution $C_{eq}(t)$. This is also supported by the fact that no ωt -scaling is observed for $\chi''(\omega, t)$. The exponent α is positive and very small; typically $\alpha = 0.07$ at $T = T_{RSG} = 3.5$ K in the RSG phase (see Table I). This value of α is considered to coincide with the exponent m for the stretched exponential relaxation. (ii) The susceptibility $\chi_{ZFC}(t)$ for $t \approx t_w$ and $t > t_w$ mainly comes from the aging contribution. As shown in Fig. 8, the exponent n depends on T and is 0.78 at $T \approx T_{RSG}$.

Ozeki and Ito⁴² have studied the nonequilibrium relaxation of the $\pm J$ Ising model in three dimensions. They have shown that $C(t_w; t + t_w)$ obeys the power-law form: $t^{-\lambda_q}$ for $t \ll t_w$ and $t^{-\lambda_{ne}}$ and for $t \gg t_w$, where $\lambda_q = 0.070(5)$ and $\lambda_{ne} = 0.175(5)$ at $T = 0.92T_{SG}$. The value of λ_q is consistent with that obtained by Ogielski:¹⁸ $\lambda_q = 0.065$ at $T = T_{SG}$. The exponent λ_{ne} characterizes the nonequilibrium relaxation. The exponent λ_q at T_{SG} is described by $\lambda_q(T_{SG}) = \beta/x$, where x is the dynamic critical exponent and β is the exponent of the SG order parameter. In the previous paper¹¹ we have reported the values of β and x as $\beta = 0.57$ and $x = 8.5$, leading to $\lambda_q = 0.067$. The agreement between the theory and experiment is very good. It is predicted that the t dependence of $\chi''(\omega, t)$ for $\omega t \gg 1$ is dominated by that of the aging part $\chi''_{ag}(\omega, t)$: $\chi''_{ag}(\omega, t) \approx (\omega t)^{-b}$ with $b = \lambda_{ne}$. Experimentally it has been confirmed that $\chi''(\omega, t)$ in the SG phase obeys the ωt -scaling law with $b = 0.14 \pm 0.03$ for $\text{Fe}_{0.5}\text{Mn}_{0.5}\text{TiO}_3$ ($T_{SG} = 20.7$ K)⁴³ and $b = 0.255 \pm 0.005$ for $\text{Cu}_{0.5}\text{Co}_{0.5}\text{Cl}_2\text{-FeCl}_3$ GBIC.⁴⁴

D. Validity of the stretched exponential relaxation

We discuss the validity of the stretched exponential relaxation. We show that $\chi_{ZFC}(t)$ can be well described by the stretched exponential relaxation with $m = 0$. However, we find that the least squares fit of the data of χ_{ZFC} vs t to the stretched exponential relaxation with $m \neq 0$ does not work well in determining the values of n and m . The value of n is very sensitive to the small change in m . In Sec. II B we assume that $\chi_{ZFC}(t)$ is given by Eq.(15). Then $S(t)$ has a peak at $x_{cr} = t_{cr}/\tau$ described by Eq.(19). As shown in the contour plot of x_{cr} in the (n, m) plane of Fig. 1(a), the value of x_{cr} strongly depends on the values of n and m . In Fig. 1(b) we show the plot of x_{cr} as a function of m for a fixed n . The value of x_{cr} takes 1 at $m = 0$ and drastically decreases with increasing m . Experimentally the value of x_{cr} is estimated from the ratio of t_{cr} to τ , where t_{cr} is the time at which $S(t)$ takes a peak and τ is from the least squares fit of the data of χ_{ZFC} vs t to the stretched exponential relaxation with $m = 0$. The ratio x_{cr} provides a good measure to determine whether the stretched exponential relaxation is valid for our system. Experimentally we find that the ratio x_{cr} is dependent on t_w and T ($3 \leq T \leq 8$ K): $x_{cr} = 0.93 \pm 0.29$ for $t_w = 1.5 \times 10^4$ sec and $x_{cr} = 1.27 \pm 0.15$ for $t_w = 3.0 \times 10^4$ sec. In our simple model, it follows that m becomes negative when $x_{cr} > 1$. Furthermore, in Sec. V C, we show that $n = 0.78$ and $m = 0.07$ at T_{RSG} . However, these values do not satisfy the inequality ($4m + n < 1$). This inequality is required for the peak of $S(t)$ to appear in the case of the stretched exponential relaxation. When $4m + n = 1$, $x_{cr} = 2^{-2/1-n}$, which is independent of m . The value of x_{cr} becomes zero as n tends to unity. In our system, $n = 0.73 - 0.81$. Using the inequality [$m < (1 - n)/4$], the upper limit of m can be estimated as 0.0475 for $n = 0.81$ (or $1 - n = 0.19$). Here we note that the exponent b for $\chi''_{ag}(\omega, t)$ [$\approx (\omega t)^{-b}$] is on the same order as the value of $(1 - n - m)$ or $(1 - n)$. In general the relationship between n and b may be derived from the relaxation rate $S(t)$ as a function t/t_w , where $t \approx t_w$ is replaced by $2\pi/\omega$.

VI. CONCLUSION

$\text{Cu}_{0.8}\text{Co}_{0.2}\text{Cl}_2\text{-FeCl}_3$ GBIC undergoes successive transitions at the transition temperatures T_c (≈ 9.7 K) and T_{RSG} (≈ 3.5 K). The FM phase of our system is characterized by the aging phenomena and nonlinear magnetic susceptibility. The relaxation rate $S(t)$ exhibits a characteristic peak at t_{cr} close to a wait time t_w below T_c , indicating the occurrence of aging phenomena in both the RSG and FM phases. The aging behavior in the FM phase is fragile against a weak magnetic-field perturbation. In the FM phase there occurs a partial rejuvenation effect in $S(t)$ under the T -shift perturbation. The time (t) dependence of $\chi_{ZFC}(t)$ around $t \approx t_{cr}$ is well approximated by a stretched exponential relaxation. The relax-

ation time τ ($\approx t_{cr}$) exhibits a local maximum around 5 K, reflecting a chaotic nature of the FM phase. It drastically increases with decreasing temperature below T_{RSG} , as is usually seen in the SG phase of SG systems.

Acknowledgments

We would like to thank H. Suematsu for providing us with single crystal kish graphite, and T. Shima and B.

Olson for their assistance in sample preparation and x-ray characterization. Early work, in particular for the sample preparation, was supported by NSF DMR 9201656.

* suzuki@binghamton.edu

- ¹ K. Jonason, J. Mattsson, and P. Nordblad, Phys. Rev. Lett. **77**, 2562 (1996).
- ² K. Jonason, J. Mattsson, and P. Nordblad, Phys. Rev. B **53**, 6507 (1996).
- ³ K. Jonason and P. Nordblad, J. Mag. Mag. Mater. **177-181**, 95 (1998).
- ⁴ K. Jonason and P. Nordblad, Eur. Phys. J. B **10**, 23 (1999).
- ⁵ P.D. Mitchler, R.M. Roshko, and W. Ruan, Phil. Mag. B **68**, 539 (1993).
- ⁶ D. Li, R.M. Roshko, and G. Yang, Phys. Rev. B **49**, 9601 (1994).
- ⁷ E. Vincent, V. Dupuis, M. Alba, J. Hammann, and J.-P. Bouchaud, Europhys. Lett. **50**, 674 (2000).
- ⁸ E. Vincent, F. Alet, M. Alba, J. Hammann, M. Ocio, and J.P. Bouchaud, Physica B **280**, 260 (2000).
- ⁹ V. Dupuis, E. Vincent, M. Alba, and J. Hammann, Eur. Phys. J. B **29**, 19 (2002).
- ¹⁰ K. Motoya, H. Hioki, and J. Suzuki, J. Phys. Soc. Jpn. **72**, 3212 (2003).
- ¹¹ M. Suzuki and I.S. Suzuki, Phys. Rev. B **69**, 144424 (2004).
- ¹² L. Lundgren, in *Relaxation in Complex Systems and Related Topics*, edited by I.A. Campbell and C. Giovannella (Plenum Press, New York, 1990) p.3.
- ¹³ D.S. Fisher and D.A. Huse, Phys. Rev. B **38**, 373 (1988); **38**, 386 (1988).
- ¹⁴ E. Vincent, J. Hammann, M. Ocio, L.-P. Bouchaud, and L. F. Cugliandolo, in *Complex Behavior of Glassy Systems*, edited by M. Rubí and C. Pérez-Vicente (Springer Verlag, Berlin, 1997) p.184.
- ¹⁵ T. Komori, H. Yoshino, and H. Takayama, J. Phys. Soc. Jpn. **68**, 3387 (1999); **69**, 1192 (2000); **69**, Suppl. A, 335 (2000).
- ¹⁶ M. Picco, F. Ricci-Tersenghi, and F. Ritort, Eur. Phys. J. B **21**, 211 (2001).
- ¹⁷ L. Berthier and J.-P. Bouchaud, Phys. Rev. B **66**, 054404 (2002).
- ¹⁸ A.T. Ogielski, Phys. Rev. B **32**, 7384 (1985).
- ¹⁹ G.J.M. Koper and H.J. Hilhorst, J. Phys. France **49**, 429 (1988).
- ²⁰ R.V. Chamberlin, G. Mozurkewich, and R. Orbach, Phys. Rev. Lett. **52**, 867 (1984).
- ²¹ R. Hoogerbeets, W.-L. Luo, and R. Orbach, Phys. Rev. Lett. **55**, 111 (1985).
- ²² R. Hoogerbeets, W.-L. Luo, and R. Orbach, Phys. Rev. B **34**, 1719 (1985).
- ²³ M. Alba, M. Ocio, and J. Hammann, Europhys. Lett. **2**, 45 (1986).
- ²⁴ L. Lundgren, P. Nordblad, and P. Svedlindh, Phys. Rev. B **34**, 8164 (1986).
- ²⁵ M. Alba, J. Hammann, M. Ocio, Ph. Refregier, and H. Bouchiat, J. Appl. Phys. **61**, 3683 (1987).
- ²⁶ P. Granberg, P. Svedlindh, P. Nordblad, and L. Lundgren, Phys. Rev. B **35**, 2075 (1987).
- ²⁷ P. Nordblad, L. Lundgren, P. Svedlindh, L. Sandlund, and P. Granberg, Phys. Rev. B **35**, 7181 (1987).
- ²⁸ R. Hoogerbeets, W.-L. Luo, and R. Orbach, Phys. Rev. B **35**, 7185 (1987).
- ²⁹ D. Chu, G.G. Kenning, and R. Orbach, Phys. Rev. Lett. **72**, 3270 (1994).
- ³⁰ D. Chu, G.G. Kenning, and R. Orbach, Phil. Mag. B **71**, 479 (1995).
- ³¹ L.W. Bernardi, H. Yoshino, K. Hukushima, H. Takayama, A. Tobo, and A. Ito, Phys. Rev. Lett. **86**, 720 (2001).
- ³² M. Suzuki and I.S. Suzuki, cond-mat/0308285; Eur. Phys. J.B, submitted (2003).
- ³³ D. Sherrington and S. Kirkpatrick, Phys. Rev. Lett. **32**, 1792 (1975).
- ³⁴ H. Takayama, J. Magn. Magn. Mater. **272-276**, 256 (2004).
- ³⁵ P.E. Jönsson, H. Yoshino, and P. Nordblad, Phys. Rev. Lett. **89**, 097201 (2002).
- ³⁶ P.E. Jönsson, H. Yoshino, and P. Nordblad, Phys. Rev. Lett. **90**, 059702 (2003).
- ³⁷ J. Hammann, M. Ocio, and E. Vincent, in *Relaxation in Complex Systems and Related Topics*, edited by I.A. Campbell and C. Giovannella (Plenum Press, New York, 1990) p.11.
- ³⁸ S.F. Edwards and P.W. Anderson, J. Phys. F **5**, 965 (1975).
- ³⁹ G. Parisi, Phys. Rev. Lett. **43**, 1754 (1979).
- ⁴⁰ G. Toulouse, J. Phys. (France) Lett. **41**, L447 (1980).
- ⁴¹ G. Aeppli, S.M. Shapiro, R.J. Birgeneau, and H.S. Chen, Phys. Rev. B **28**, 5160 (1983).
- ⁴² Y. Ozeki and N. Ito, Phys. Rev. B **64**, 024416 (2001).
- ⁴³ V. Dupuis, E. Vincent, J.-P. Bouchaud, J. Hammann, A. Ito, and H. Aruga Katori, Phys. Rev. B **64**, 174204 (2001).
- ⁴⁴ I.S. Suzuki and M. Suzuki, Phys. Rev. B **68**, 094424 (2003).